Discrete *vs* continuous controversy in physics

Annick LESNE
Laboratoire de Physique Théorique des Liquides, Case 121
4 Place Jussieu, 75252 Paris Cedex 05, France
lesne@lptl.jussieu.fr

This paper presents a sample of the deep and multiple interplay between discrete and continuous behaviors and corresponding modelings in physics. The aim of this overview is to show that discrete and continuous features coexist in any natural phenomenon, depending on the scales of observation. Accordingly, different models, either discrete or continuous in time, space, phase space or conjugate space can be considered. Some caveats about their limits of validity and their interrelations (discretization, continuous limits) are pointed out. Difficulties and gaps arising due to the singular nature of continuous limits and to information loss accompanying discretizations are discussed.

I. INTRODUCTION: SETTING THE STAGE

This special issue of *MSCS* reflects the deep and multiple debates arising in pure and computational mathematics about discrete *vs* continuous frameworks and computations. The debated issues are ranging from practical caveats about the use of discrete computational schemes for solving continuous equations, or continuous frameworks to describe discrete systems, up to conceptual questions about the very nature, either discrete or continuous, of the reality (rather of our perception of the reality). The tension between discrete and continuous aspects is also ubiquitous in physics. In this contribution, I'll try to give a brief and unavoidably far from complete account of the numerous facets of this dilemma, from a physical viewpoint, with as less prerequisites as possible.

A. The terms of the debate: "discrete" and "continuous"

Let us first clarify the discussion and sketch the skeleton on which specific examples will be articulated. The preliminary step is to agree on the terms of the debate. Discrete (respectively continuous) can refer to:

— *time*: the evolution of a system can be described either as a continuous trajectory in the space of system states (what is called the "phase space"), either as a discrete sequence of successive states (see Section II);

— *real space*: the underlying space (of dimension $d = 1, 2, 3$ in natural situations or possibly larger in theoretical case studies) might be seen either as a continuum, where positions are labeled by d real-valued coordinates, either as a tiling of discrete cells, or equivalently a lattice, where positions are labeled by d integers (see Section III);

— *phase space*: the representation of the system state may scan a continuum (a vector space or a manifold) or vary inside a discrete set (finite or countable) of configurations (see Section IV);

— *conjugate space*, in the context of spectral analyses: we shall see in Section V that spectra offer another modality of the "discrete *vs* continuous" alternative.

It is to note that the meaning of "continuous" is less ambiguous in physics than in mathematics, where set-theoretic, topological and measure-theoretic notions of continuity superimpose. In physics, the required smoothness is included in the very notion of continuous medium and in the same way, a continuous dynamical system will be differentiable unless explicitly mentioned. It might have seemed sensible to distinguish between *discrete* systems, namely made of disjoint (seemingly intrinsic) particles, and *discretized* systems, resulting from a (seemingly arbitrary) partition; examples of quantum particles, localization and pattern formation (Section III), or symbolic dynamics (Section IV), will show that such a distinction might in fact be irrelevant.

B. The debated questions

The debate itself stands at different levels:

— it might concern *computational techniques*, for instance discrete numerical schemes used to implement continuous equations, or continuous limits replacing an exact discrete formula by an approximate but tractable one;

— it might refer to the choice of the *proper framework to model* the system according to the phenomenon of interest and the description (or observation) scale;

— it might finally consider the *nature of the phenomenon*, and investigate the observable consequences of the discrete nature of any actual material (made of atoms) and the quantum nature (discrete low-energy levels) of these atoms or, on the contrary, investigate whether the underlying continuous wave function of the system is essential to understand its behavior. This third facet of the debate partly vanishes in the now acknowledged ambivalent picture of, say, an electron *jointly* as a particle and as a wave, and we'll see that similar ambivalent pictures are also the rule at higher scales, in classical physics.

II. DISCRETE *VS* CONTINUOUS IN TIME

In this section, I present some examples illustrating the relations between discrete-time and continuous-time dynamic modelings. The focus will be on difficulties that can arise, either in theoretical modeling (Secs. II A, II B, II C), data analysis (Sec. II D) or numerical implementation (Sec. II E), when trying to bridge discrete and continuous viewpoints.

A. Poincaré sections

A now acknowledged discretization procedure of a continuous dynamical system is provided by Poincaré sections (see Fig. 1). This procedure has been deviced by Poincaré in the context of celestial mechanics, in the aim of reducing the analysis of long-term planetary motion and its dynamic stability [Poincaré 1892].

Let us consider an autonomous differentiable dynamical system $\dot{z} = V(z)$, generating a flow $\Phi(z,t)$ and possessing a *periodic orbit* $\mathcal{O}$ of period T. The behavior of the flow in the neighborhood of $\mathcal{O}$ can be tracked through the successive intersections of the flow with an hypersurface Σ (for instance the locus of points sharing a common phase) crossing $\mathcal{O}$ *once and transversally* at $x^* \in \Sigma$. One thus defines the *return map* φ_Σ (or *Poincaré map*) in an appropriate neighborhood U of x^* in Σ: the point $x_1 = \varphi_\Sigma(x_0)$ is the first intersection with Σ of the trajectory $t \to \Phi(x_0,t)$ starting from $x_0 \in U$, and the time $\tau(x_0)$ at which the intersection occurs (i.e. such that $\Phi(x_0,\tau(x_0)) = \varphi_\Sigma(x_0) = x_1$) is called the *return time* [Guckenheimer et Holmes 1983]. By construction, $\varphi_\Sigma(x^*) = x^*$, i.e. x^* is a fixed point of the Poincaré map and $\tau(x^*) = T$.

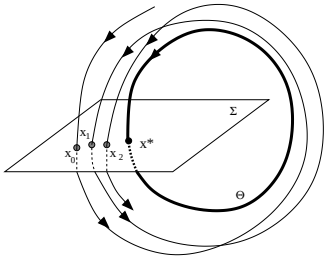

FIG. 1. Poincaré section discretization method. The periodic orbit $\mathcal{O}$ is underlined in bold. The successive intersections x_0, x_1, x_2, ... of a continuous trajectory with the section Σ define the return map φ_Σ through $x_1 = \varphi_\Sigma(x_0)$, $x_2 = \varphi_\Sigma(x_1)$, and so on.

The rationale of this discretization is the qualitative similarity between the behavior of the discrete evolution generated by φ_Σ in Σ and the behavior of the original (continuous) flow, in particular in what regards the stability of the periodic orbit $\mathcal{O}$, identical to the stability of its trace x^* under the action of the Poincaré map φ_Σ. The correspondence is even quantitative, as we shall see now. Linearizing the continuous dynamical system $\dot{z} = V(z)$ around the periodic orbit $\mathcal{O}$ yields an equation $\dot{u} = DV[\Phi(z,x^*)].u$ whose solutions are of the form $u(t) = u_0(t)e^{tR}$, with $u_0(t+T) = u_0(t)$ for any t and R a matrix. The eigenvalues $(\Lambda_j)_j$ of the constant matrix e^{TR} are called the *Floquet multipliers* of the orbit $\mathcal{O}$. The multiplier associated with perturbations along the orbit $\mathcal{O}$ is $\Lambda_0 = 1$; the moduli of the remaining ones determine the stability of $\mathcal{O}$ (stable if all are smaller than 1). It is straightforward to show that the eigenvalues $(\lambda_j)_j$ of the Jacobian matrix $D\varphi_\Sigma(x^*)$ of φ_Σ in x^* (also called the stability matrix of the fixed point x^*) are related to the Floquet multipliers according to $\Lambda_j = e^{\lambda_j T}$ (letting apart $\Lambda_0 = 1$) [Guckenheimer and Holmes 1983]: the (in)stability of x^* with respect to the discrete Poincaré dynamics is thus equivalent to the (in)stability of the periodic orbit $\mathcal{O}$ with respect to the original continuous dynamics. The multipliers $(\Lambda_j)_j$ are characteristics of the periodic orbit as a whole, hence do not depend on the specific intersection point x^*; in consequence, *changing the section Σ would not modify the exponents $(\lambda_j)_j$), neither the stability properties derived from the analysis of the discrete dynamics.*

In this method, the discretization step is not arbitrarily chosen but prescribed by the dynamics. The main virtue of a Poincaré section is indeed to provide an *intrinsic discretization*, lowering the phase space dimension by at least one unit, adapted to the dynamics (the time step $\tau(x_0)$ depends on the considered trajectory). It captures some *generic features* of the continuous flow, e.g. perturbations modifying trajectories outside Σ are of no consequences if the intersections with Σ are preserved. It is thus a first step to bring out the geometry of the dynamics and its universal properties.

An important caveat is the *restricted range of validity* (in the phase space) of this discretization: the return map is defined only in a neighborhood U of the periodic orbit $\mathcal{O}$ (that should intersect only once Σ). Smoothness of the flow in U is also essential. It is most often satisfied, ensuring a wide range of application of the Poincaré section method. In some special instances, it might nevertheless happen that the return time $\tau(x)$ is not bounded above and below in U, and the Poincaré map then fails to reflect quantitatively the behavior of the flow: if $\tau(x)$ does not remain in a finite interval $[\tau_m, \tau_M]$ (with $\tau_m > 0$ and $\tau_M < \infty$) for any $x \in U$, the time correlation functions of the discrete and continuous flows strongly differ, and accordingly their Fourier transforms (what is called the power spectra, see Sec. V C) exhibit different behaviors. For instance, divergence of $\tau(x)$ makes the correlation time of the continuous flow to diverge even if the correlation function of the discrete evolution is well-behaved, i.e. decreases exponentially with a finite characteristic time. The way out this difficulty is to keep track of the return time function $x \to \tau(x)$. In this aim, a new mathematical object has been introduced, known as a *special flow* (or "flow under the function $\tau(x)$", or "flow over the map $\varphi_\Sigma(x)$"). It is a continuous-time dynamics $[x(t), y(t)]$, with a step-wise constant component $x(t)$ (associated with the Poincaré map) varying in the Poincaré section Σ and the other one $y(t)$ taking real positive values. It is defined recursively as follows: starting from $(x_0, 0)$ at time $t = 0$, the second component y steadily increases with velocity 1 until it reaches the value $\tau(x_0)$, at time $t = \tau(x_0)$; then the trajectory jumps from $[x_0, \tau(x_0)]$ to the point $[x_1 \equiv \varphi_\Sigma(x_0), 0]$; then the second component steadily increases with velocity 1 until it reaches the value $\tau(x_1)$, at time $t = \tau(x_0) + \tau(x_1)$; then the trajectory jumps from $[x_1, \tau(x_1)]$ to the point $[x_2 \equiv \varphi_\Sigma^2(x_0), 0]$, and so on. Such a flow bridges the dynamics generated by the Poincaré map, too reduced in the singular cases considered here, and the original continuous one: the spectral properties (i.e. time correlations) of the special flow matches those of the continuous dynamics [Zaks and Pikovsky 2003].

B. Billiards and Birkhoff maps

A special instance of Poincaré maps is encountered in billiards (see Fig. 2). The motion of a tracer point-particle inside the billiard is an alternation of free flights and elastic reflections on the boundaries: in consequence the phase space is of dimension $d = 3$ for a billiard in the plane, since the modulus of the particle velocity remains constant. The dynamic recursion is fully determined by the knowledge of collisions, namely by the map relating a pre-collisional state to the next one, known as the *Birkhoff map* [Gaspard 2004a]. It corresponds to the Poincaré map associated with the section containing the particle states $\{(\vec{r}, \vec{v})\}$ with $\vec{r}$ located on the boundary and $\vec{v}$ the incoming velocity. The return time is equal to the free flight duration, hence depends on the overall shape of the billiard (and on general on the boundary point where reflection occurs). The Birkhoff map critically depends on the local geometry of the boundary: for instance, a convex boundary (e.g. a disk) is defocusing and amplifies any incident inhomogeneity or fluctuation, generically leading to chaos if iterated in a bounded domain, as in the Sinai's billiard represented on Fig. 2 (left).

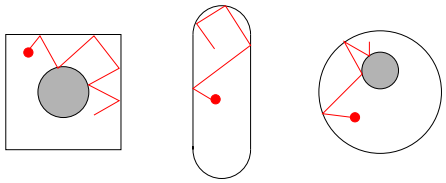

FIG. 2. Three examples of chaotic billiards: (left) Sinai's billiard, (middle) Bunimovich's stadium, (right) when the outer square wall of the Sinai's billiard is replaced by a circular wall, the inner disk should be eccentric in order to get chaos.

C. Discrete models

Discrete models can also be introduced directly, for instance in population dynamics where each time label corresponds to a generation. Let us consider the formal example: $x_{n+1} = x_n + hg(x_n)$ in order to underline a key point: the comparison with a continuous counterpart $dx/dt = ag(x)$ over a duration h_0 shows that the parameter $h = ah_0$ jointly accounts for the instantaneous growth rate a and for the delay h_0 that takes place between the action $ag(x_n)$ and its consequence on the following state x_{n+1}. It is thus not surprising that h appears as a control parameter of

the behavior. Oscillations might appear at large enough values of h if g is nonlinear, typically when the delay h_0 overwhelms the characteristic growth time $1/a$. This point is worked out on detailed examples in the contribution by H. Krivine et al. in this volume, where it is shown to give a qualitative, and even quantitative understanding of the instabilities arising in the numerical (hence discrete) implementation of continuous dynamics (see also Sec. II E).

More generally, it is to be kept in mind that dynamical system modeling, e.g. for chemical reactions, accounts for time lags *through kinetic rates of memoryless evolution equations*. This is technically most fruitful, but might sometimes erase the actual mechanisms, e.g. the interplay between delays and characteristic times, or the kinetic race between competing chemical pathways. Alternative approaches have been developed, such as delay equations, integro-differential equations involving a memory kernel or, technically more tractable in complex systems, a logical circuit analysis [Thomas and Kaufman 2001].

D. Nyquist theorem on experimental sampling frequency

On the experimental side, concrete bounds imposed by time resolution of the recording apparatus are described by an important theorem of signal analysis, the *Nyquist theorem* [Nyquist 1928] [Shannon 1949]. Sampling frequency puts a limit on the variations that can be followed: obviously, variations occuring faster than the sampling frequency, hence taking place between two successive recordings, cannot be tracked. Nyquist theorem makes quantitative this quite intuitive statement: *full experimental determination of a time signal $f(t)$ containing no frequencies higher than ω_m requires to sample the signal with a time resolution $\tau \leq \tau_m = \pi/\omega_m$*. To be more precise, the case of discrete sampling (when the apparatus needs to relax between successive measurements) should be distinguished from the case of local averaging (when the overwhelming lag comes from the time integration performed by the apparatus to deliver a value), which reflects in a factor of 2 in the above bound.

E. Euler discretization schemes

Numerical resolution of continuous equations $dX/dt = g(X)$ is generally implemented using finite difference methods, for instance the (first-order) *Euler discretization scheme* $x_{n+1} = x_n + hg(x_n)$ with $x_n \approx X(t_n = nh)$. In this context of numerical analysis, the relation between discrete-time and continuous-time dynamics is well controlled and harmless provided that the continuous evolution has characteristic times bounded below by $2\tau_m$ and the discretization step h remains below τ_m, in agreement with Nyquist theorem, Sec. II D. Higher-order schemes involve higher-order Taylor expansion of the (integrated) continuous evolution law $X(t_n + h) = X(t_n) + \int_0^h g[X(s)]ds$, leading to the following recursion at order 2: $x_{n+1} = x_n + hg(x_n) + h^2 g(x_n)g'(x_n)/2$. Using these higher-order schemes allows to relax the bound h_c on the time step up to which the numerical scheme is "stable", in the sense that its discrete-time solution interpolates the continuous one. The stability threshold $h_c(n)$ of the Euler scheme of order n increases with n up to infinity. Implicit schemes can be used to cure the numerical instability of direct schemes (they actually correspond to a direct scheme of infinite order): basically, the idea is to solve the recursion: $x_{n+1} = x_n + hg(x_{n+1})$ instead of: $x_{n+1} = x_n + hg(x_n)$ in order to reconstruct the continuous solution of $dX/dt = g(X)$. The price to pay is that these implicit schemes are far less tractable numerically. A basic example is detailed in the contribution by H. Krivine et al. in this volume. Another well-known example of misleading discretization is provided by the Verlet time-discretization for the pendulum: one obtains the standard map ($I_{n+1} = I_n + K \sin\theta_n, \theta_{n+1} = \theta_n + I_{n+1}$) whose control parameter K is proportional to the discretization step h. For $h > h_c$, it is chaotic while the original system is regular.

III. DISCRETE *VS* CONTINUOUS IN REAL SPACE

The discussion about discrete or continuous time variables presented in the previous section should naturally be supplemented with a similar discussion regarding real-space variables. Issues range from the nature of a particle (Secs. III A and III G) to the status of lattice models (Sec. III B), caveats about continuous limit (Secs. III C, and III D) or the origin and modeling of localization (Secs. III E and III F).

A. From molecular chaos to continuous media

In classical physics, an important paradigm bridging the discrete structure of any material, made of atoms or molecules and a continuous description is the *continuous medium approximation*. It corresponds to a mesoscopic modeling of a many-particles system extended in space, for instance a fluid, starting with a partition of the real space into cells of linear size a (it is noticeable that the passage from a cloud of particles to a continuous medium begins with a real-space discretization). The main assumption is that a is large compared to the microscopic scales (e.g. the mean free path of the molecules) but small compared to the macroscopic scales (e.g. the characteristic length associated with density or temperature gradients). In particular, each cell should contain a large number of particles: $\rho a^d \gg 1$ if ρ is the number density of the fluid and d the real-space dimension. An argument based on the law of large numbers, itself rooted in an assumption of molecular chaos preventing long-range correlations between the molecules (see Fig. 3), supports a continuous description of the medium at the cell level: any observable $\mathcal{A}$ will be associated with a *smooth* and *deterministic* field $A(\vec{r},t)$, where $A(\vec{r},t)$ is the value of $\mathcal{A}$ averaged at time t over the cell located in $\vec{r}$. For instance in hydrodynamics A will be either the density, velocity or temperature field [Landau and Lifschitz 1984].

This description emerges from a full statistical picture describing the N-particle system through its distribution function f_N such that $f_N(\vec{r}_1,\vec{v}_1,\ldots,\vec{r}_N,\vec{v}_N,t)d^d\vec{r}_1 d^d\vec{v}_1 \ldots d^d\vec{r}_N d^d\vec{v}_N$ is the probability that for each $j=1,\ldots,N$, the particle j lies in the elementary volume $d^d\vec{r}_j \sim a^d$ around $\vec{r}_j$ with a velocity lying in the elementary volume $d^d\vec{v}_j$ around $\vec{v}_j$ (where again d is the dimension of the real space, i.e. currently $d=3$). The time evolution of this distribution function is ruled by the Liouville equation following from the deterministic Newton dynamics for the N particles. The following steps are to integrate over $N-1$ particles, then to use the Boltzmann approximation $f_2(\vec{r}_1,\vec{v}_1,\vec{r}_2,\vec{v}_2,t) \approx f_1(\vec{r}_1,\vec{v}_1)f_1(\vec{r}_2,\vec{v}_2)$ (again supported by the decorrelation achieved by molecular chaos) to express the evolution of $f_1(\vec{r}_1,\vec{v}_1)$ in a closed form (i.e. involving only f_1) and finally integrating out the velocity $\vec{v}_1$ to get the density $n(\vec{r},t)$, the velocity field $\vec{u}(\vec{r},t)$ and the temperature $T(\vec{r},t)$ [Dorfman 1999]:

$$n(\vec{r},t) = \int f_1(\vec{r},\vec{v})d^d\vec{v}, \qquad \vec{u}(\vec{r},t) = \frac{1}{n(\vec{r},t)}\int \vec{v} f_1(\vec{r},\vec{v})d^d\vec{v}, \qquad T(\vec{r},t) = \frac{1}{d\, k_B\, n(\vec{r},t)}\int \frac{mv^2}{2} f_1(\vec{r},\vec{v})d^d\vec{v} \quad (1)$$

This description is generally supplemented with an hypothesis of *local thermodynamic equilibrium*, in each cell, allowing to use all the thermodynamic relations at each point $\vec{r}$. The simplest example is the description of transport phenomena, e.g. diffusion equation $\partial_t n = D\Delta n$ (where Δ denotes the Laplacian) starting from deterministic molecular dynamics [Laguës and Lesne 2003]. Work is still in progress to extend such an effective continuous mesoscopic description to far-from-equilibrium systems, the main open issue being to define entropy and temperature on microscopic bases [Gruber et al. 2004].

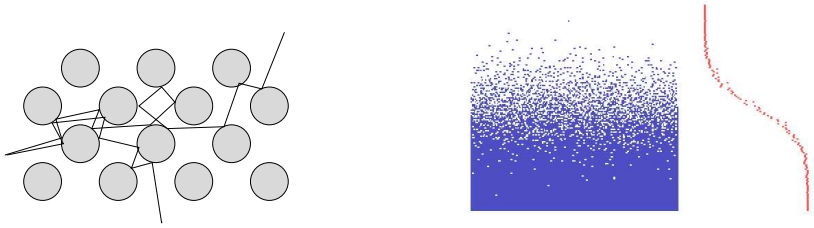

FIG. 3. (Left) microscopic deterministic model of diffusive transport (Lorentz gas model, initially developed as a classical model of electron transport in the lattice formed by the atomic nuclei [Dorfman 1999]) where a light particle experiences numerous elastic collisions on circular scatterers (grey disks). Defocusing character of the collisions induces molecular chaos, in turn generating a diffusive motion and supporting a statistical approach. (Right) observation at time t of the microscopic simulation (implementing discrete random walks) of diffusion in a semi-infinite box, starting from a step in $x=0$ at time 0. (Extreme right) average profile $n(x,t)$ (vertical axis represents the spatial coordinate x whereas concentration $n(x,t)$ spans values from 0 to 1 horizontally); $n(x,t)$ tends to the solution of the 1-dimensional diffusion equation $\partial_t n = \partial^2_{xx} n$ as the number of particles tends to infinity.

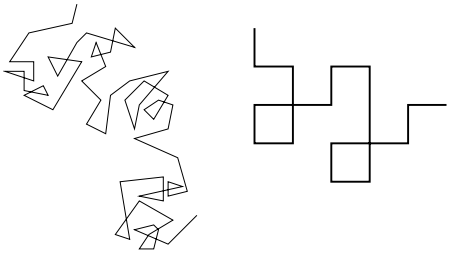

FIG. 4. Lattice approximation (right) of a Brownian trajectory (left). The associated dynamic model is a lattice random walk (Markov chain) fully prescribed by the probability to jump from any node to one of its nearest neighbors on the lattice.

B. Lattice models

Conversely, continuous models might be reduced, e.g. for computation or simulation purposes, into lattice models, where the underlying real space is a regular lattice. Three main examples are illustrated on Figs. 4, 5, and 6, namely Brownian motion on a lattice, random-walk modeling of polymer chain conformations and percolation theory, e.g. for porous media and other disordered systems. Let us briefly discuss the main discrepancies arising between lattice models and actual systems, and the situations where lattice models are relevant.

The discretization is all the more perceptible as the relative size L/a is small (a being the linear cell size and L the linear lattice size). The continuous limit corresponds to $a/L \to 0$. A strong lattice effect might originate in the restricted symmetry properties of the lattice: translational invariance is replaced by invariance under translations of step equal to an integer multiple of a (we here recover the criterion of validity $a \ll L$). Isotropy breaks down and is replaced by invariance under the action of finite groups of rotations (those encountered in the natural lattice structures of crystals).

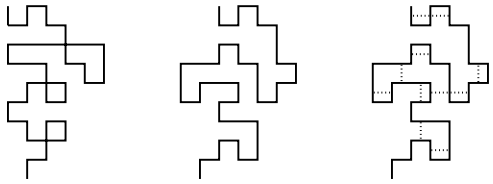

FIG. 5. Lattice models of polymers. (Left) Brownian random walk, with no correlations between successive steps; the size a of a step (a "monomer") should be larger than the persistence length of the actual polymer chain, so that all relative orientations are possible. (Middle) steric hindrance between successive monomers is taken into account in a more refined model, known as *self-avoiding walk*; it exhibits an infinite memory since the walker remembers all the previously visited nodes in order to avoid them. (Right) a third model, the interacting self-avoiding walk, accounts for short but finite range interactions between monomers: self-avoidance (infinite repulsion between monomers at the same point) is here supplemented by an interaction $-J$ (attractive if $J > 0$) between any neighboring steps (i.e. monomers) on the lattice (dotted lines).

Using lattice models is especially relevant when investigating *universal properties*, i.e. properties common to physical systems of very different natures but sharing the same geometrical properties and symmetries. Let us consider for instance percolation models (see Fig. 6). A remarkable feature is the percolation transition, i.e. the emergence of an infinite cluster spanning the whole system, above a threshold $p = p_c$. This transition appears to be closely analog to a second-order phase transition and it accordingly satisfies scaling laws; for instance, the correlation length ξ obeys: $\xi(p) \sim |p - p_c|^{-\nu}$. The value p_c of percolation threshold depends on the lattice geometry (e.g. it differs for a square lattice and a triangular lattice) but the exponents involved in the scaling laws, such as ν, depend only on the space dimension and percolation type [Laguës and Lesne 2003]. In the same spirit, universal properties of diffusion support its implementation with discrete random walks: the exponent γ involved in the diffusion law $R(t) \sim t^{\gamma/2}$ will not depend on the lattice geometry (provided the lattice remains regular). One may go further and show, using renormalization methods [Lesne 1998], that *universal properties are identical in continuous systems and in their discretized versions*; the latter will be preferred for obvious simplicity reason in theoretical and still more, in numerical investigations.

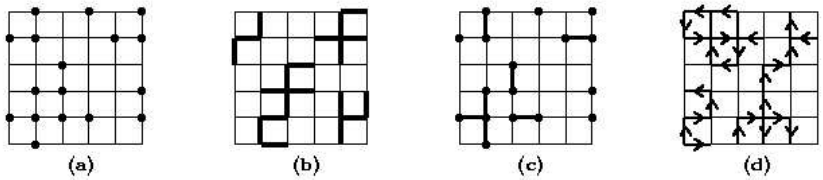

FIG. 6. Percolation models: the real space is discretized, either as a lattice of nodes (a: site percolation), a web of links (b: bond percolation), both (c: site-bond percolation) or as a web of oriented links (d: directed percolation). Each unit (node or link) is supposed to be fully described by a Boolean state variable 0 (empty) or 1 (occupied). Sites are occupied (links are present) with a probability p independently each of each other. Overall behavior (e.g. conductivity, permeability, contagion) depends on the existence of a percolating cluster, namely a connected path bridging the opposite sides of the lattice; its emergence is a critical transition, occurring for a well-defined probability p_c (*percolation threshold*) when lattice size goes to infinity [Stauffer and Aharony 1992].

C. Diffusion in a porous medium

As presented on Fig. 3, diffusion basically involves the motion of discrete particles. An operational way to get a continuous description of a diffusion process is to cast the behavior into a phenomenological description involving effective parameters accounting for all microscopic details through their integrated consequences at higher scales. Let us consider diffusion in a porous medium. Two situations are to be distinguished [Laguës and Lesne 2003]:

— either the pores have a finite typical size a. The intuitive idea is that at scales far larger than a, the medium can be considered as an homogeneous continuous medium (see Fig. 7). Mathematically well-controlled averaging procedures and homogenization theorems are then available, e.g. relating the derivatives of averaged variables and the average derivatives [Bensoussan et al. 1978]. It is thus possible to derive the spatio-temporal evolution of the locally averaged density (averaged over a representative region, far larger than a pore but still elementary compared to the whole system). The remarkable fact is that it has the same form as the plain diffusion equation. Such an homogenization procedure thus yields an effective diffusion equation with a reduced diffusion coefficient $D_{eff} < D$ accounting for the obstacles encountered by the diffusing particles (having a diffusion coefficient D in plain solvent).

— either the medium exhibits pores at all sizes (fractal substrate). The diffusion is then anomalous: $R(t) \sim t^{\gamma/2}$ with $\gamma < 1$. A relevant theoretical approach is to mimic the medium using a percolation model right at the percolation threshold, then to investigate transport on the (fractal) percolation cluster. A relation can thus be shown, relating fractal characteristics of the cluster (its fractal dimension d_f and its spectral dimension $d_s \leq d_f$) and the exponent of the diffusion law, namely $\gamma = d_s/d_f$.

This example of diffusion in a porous medium illustrates a wide-ranging conclusion: *continuous limits and effective descriptions require characteristic scales to be bounded and their validity range lies far above these bounds.*

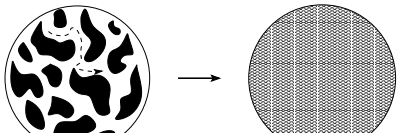

FIG. 7. Homogeneization of a diffusion process in a porous medium: particles, of diffusion coefficient D inside the pores, experience a hampered diffusive motion at larger scales; if the typical size of the pores is finite, normal diffusion is still observed, with lower diffusion coefficient D_{eff}, where D_{eff}/D is related to the medium porosity [Nicholson 2001] [Laguës and Lesne 2003]

D. Wind-tree discrete/continuous paradox

The *Lorentz-gas model* (shown on Fig. 3) is an array of circular scatterers among which a small tracer particle travels, experiencing elastic collisions at encounters with scatterers. The *wind-tree model* is quite similar, except that disks are replaced by squares (see Fig. 8). One can figure to pass from a wind-tree model to a Lorentz gas by considering, instead of squares, polygons of constant area and increasing number of sides (the well-known Archimedian limit towards a circle). It can be shown that the tracer motion is chaotic in a sufficiently dense and generic Lorentz

gas (at low densities or in special geometries, the tracer would escape along a free flight without experiencing any collisions). By contrast, the motion is not chaotic for any polygonal wind-tree model, so the question arises about the way to match these behaviors when the polygons are physically indiscernible from disks. Physically, the puzzle is solved when looking at relevant (enough large) scales: in both models, the tracer exhibits a diffusive motion. Mathematically, the way out this paradox requires to introduce an intermediary notion, adapted to the resolution ϵ, here in real space: the ϵ-entropy [Boffetta et al. 2002]. Its precise definition is given below, in Sec. IV D: it is a time entropy measuring the rate at which observation of the motion with an accuracy ϵ generates information on the trajectory. Its behavior with respect to ϵ determines the nature of the motion: $\lim_{\epsilon\to 0} h(\epsilon) = h > 0$ in case of a chaotic motion whereas $h(\epsilon) \sim 1/\epsilon^2$ in case of Brownian motion. In case of an array of polygons of side a, the tracer motion looks regular at scales $\epsilon < a$, as reflected by the values $h(\epsilon) \approx 0$, whereas it looks chaotic at scales $\epsilon > a$, according to the values $h(\epsilon) \approx const > 0$, and even diffusive at scales $\epsilon \gg a$, corresponding to a behavior $h(\epsilon) \sim 1/\epsilon^2$.

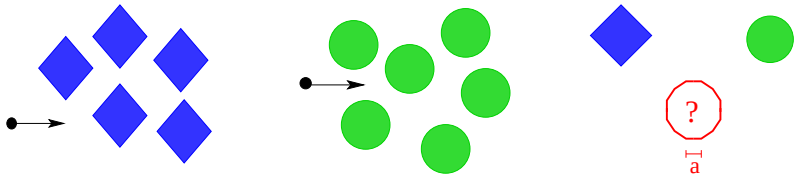

FIG. 8. (Left) wind-tree model where the motion of a tracer is non chaotic. (Middle) Lorentz gas model (see also Fig. 3) where the motion of a tracer is chaotic. (Right) what to say about polygonal scatterers when the facet size a tends to 0?

E. Localization and pattern formation

Pattern formation, namely the spontaneous appearance of well-defined shapes and patterns in an initially homogeneous system, is ubiquitous in natural sciences [Cross and Hohenberg 1993] [Murray 2002]. The emergence of discrete shapes and localized structures relates this issue to our main topic. One of the lessons of pattern formation studies, supplemented with the development of minimal models, like the set of two coupled reaction-diffusion equations introduced by Turing as a model of morphogenesis [Turing 1952], is that *localization often follows from collective effects extended in space*. It is the very presence of a spatially extended reactive substrate and nonlinear interactions that lead to a phenomenon highly localized in space and seemingly involving only a tiny, almost discrete region of the system. For instance, stripes observed in Turing structures (corresponding to roughly step-like concentration profiles for the two reactive chemical species) are actually *discrete features of an interacting whole* and they are indissolubly linked together: it is impossible to isolate, or even to modify one band without modifying another one, and the system can only be regulated as a whole. Such an example illustrates the ambivalent nature, both discrete (in their expression) and continuous (in their mechanisms) of most dynamic patterns encountered in natural sciences.

F. Localization and Dirac "generalized function"

On a more abstract level, localization provides a tractable example of the mathematical idealization currently at work in physical modeling. Point particles or the position of some event spatially localized in x_0 are currently described by a Dirac "function" $\delta(x - x_0)$. It is actually a generalized function, well defined in the framework of the theory of distributions developed by Schwartz. Its physical meaning follows from the limiting behavior (weak convergence) of peaks of increasing height, decreasing width and constant area:

$$\delta(x - x_0) = \lim_{a\to 0} \frac{1}{\sqrt{2\pi a}}\, e^{-\frac{(x-x_0)^2}{2a}} \tag{2}$$

In practice, a unimodal distribution centered in x_0 can be identified with $\delta(x - x_0)$ as soon as its width satisfies $a \ll \delta x_{obs}$ where δx_{obs} is the experimental resolution. Dirac distribution is the mathematical idealization of "point mass" so currently used in physics. Its interest for physicists is to endow current physical reasoning with mathematical rigor. From a mathematical viewpoint, its achievement is to unify entities of seemingly different mathematical natures (functions and measures) within a comprehensive theory, in which objects are defined, not in themselves, but through their actions on "probes", namely test-functions (the basic idea of weak convergence). Remarkably, this property is shared with our physical access to real world.

Another example is provided by the time analog of a point mass, namely an *instantaneous impulse*. This ideal event corresponds to an infinite force applied during a vanishing time duration. This event can be physically substantiated in the same way, by considering the limiting behavior associated with a large force applied during a short duration, when the force and the inverse duration tend to infinity in a concerted way, namely with a fixed ratio.

In the same spirit, *nonstandard analysis* allows to handle limiting behaviors in a more transparent way. It suppresses the qualitative gap between finite and limiting quantities arising when taking a limit $\epsilon \to 0$, by introducing an explicit "extension of the mathematical world", giving a mathematical status to infinitely small quantities and replacing qualitative shades by a well-defined ordering between these infinitely small quantities [Diener and Diener 1995].

G. Discrete *vs* discretized systems

It now appears that there is no reason to make a fundamental distinction between *discrete* and *discretized* systems: an object seems to be intrinsically discrete, even isolated, only if we choose the proper glasses. Let us consider for instance an atom: at very small scales, those of quantum mechanics, this "particle" is delocalized. The dilemma yet appears in the classical framework: at long time scales, we do not record a single position of the particle but rather its distribution of probability in the whole space; we might speak of "the position" of the particle only if the width of this distribution is smaller than the relevant spatial scales (e.g. observation scales or interaction ranges). Hence, discrete objects are not really more "objective" than an arbitrary chosen partition of the space in cells.

IV. DISCRETE *VS* CONTINUOUS IN PHASE SPACE

A. From agent-based descriptions to continuous models

The relation between agent-based descriptions, right at the level of individuals, and kinetic continuous-state descriptions is an ubiquitous issue, encountered for instance in population dynamics [Auger and Roussarie 1994], more generally in studying the emergence of any collective behavior ranging from granular media [Ernst 2000] to swarms, flocks or societies [Vicsek 2001], and finally at a far different scale in the context of chemical reactions [Arnold 1980]. It has been deeply investigated [Kirkpatrick and Ernst 1991] [Chopard and Droz 1998] [Droz and Pekalski 2004] to legitimate both kinetic theories of intrinsically discrete systems and discrete simulations (cellular automata) of continuous equations. It is interesting to derive explicitly such a *relation between discrete-state microscopic description and continuous-state macroscopic one*, in order to bring out the approximations lying behind kinetic continuous (real-valued) modeling [Givon et al. 2004].

Let us detail the example of the celebrated Lotka-Volterra (predator-prey) model of population dynamics, also discussed in the contribution by H. Krivine et al. in this volume:

$$\begin{cases} \dfrac{dx}{dt} = x(a - by) \\ \\ \dfrac{dy}{dt} = y(cx - d) \end{cases} \tag{3}$$

where x and y describe the respective populations of preys and predators.

The first assumption is *(H1) an assumption of spatial homogeneity* of the population, justified if the environment is itself homogeneous and species free to move and mix. It allows to neglect any space dependence and to consider only variation in time of the prey and predator populations. Let $X(t)$ and $Y(t)$ be integers describing the respective numbers of preys and predators at time t. In agent-based simulations, it is possible to describe the behavior of each agent with much details, but in analytic or cellular automata approaches, only a minimal, birth-and-death modeling is retained and the populations will evolve according to simple probabilistic rules.

Here comes a second assumption, namely the *(H2) Markov character of the evolution*. Even in a continuous-time dynamics, description implicitly involves a minimal time scale (the "size" of dt), and validity of the Markov assumption

requires dt to be larger than the "memory" of the system*. The model is thus entirely determined by a transition rate matrix W:

$$\frac{dP(X,Y,t)}{dt} = \sum_{X'} \sum_{Y'} W(X,Y|X',Y')P(X',Y',t) \tag{4}$$

where the sum runs over all positive integers X' and Y', and

$$\sum_{X} \sum_{Y} W(X,Y|X',Y') = 0 \tag{5}$$

to ensure the conservation of probability ($\sum_X \sum_Y P(X,Y,t) = 1$). Equation (4) requires an additional assumption of differentiability of $t \to P(X,Y,t)$ (*(H3) no jump, bounded transition rates*). The fourth assumption is *(H4) to identify macroscopic variables with statistical averages* $\langle X \rangle$ and $\langle Y \rangle$. This assumption is the core of the passage from a microscopic model to a macroscopic one. It is straightforward from (4) to write the time evolution of the various moments, for instance

$$\frac{d\langle X^n \rangle}{dt} = \sum_{X'} \sum_{Y'} \sum_{X} X^n \; W(X,Y|X',Y')P(X',Y',t) \tag{6}$$

At this stage, we must turn to a specific expression of W to go further. At short time scales, it is justified to suppose that *(H5) only single events will occur with a non negligible rate*, hence we accordingly consider only the following elementary transitions in W:

– birth of a prey: $(X,Y) \to (X+1,Y)$, at a rate $a_0 X$,

– capture of a prey: $(X,Y) \to (X-1,Y)$, at a rate $b_0 XY$,

– birth of a predator: $(X,Y) \to (X,Y+1)$, at a rate $c_0 XY$,

– natural death of a predator: $(X,Y) \to (X,Y-1)$, at a rate $d_0 Y$.

from which follows the expression of non-vanishing components of W:

$$W(X+1,Y|X,Y) = a_0 X W(X-1,Y|X,Y) = bX_0 Y \tag{7}$$

$$W(X,Y+1|X,Y) = c_0 XY W(X,Y-1|X,Y) = d_0 Y \tag{8}$$

Here again the assumption of the population homogeneity is essential: for instance, each prey gives rise with the same rate a_0 to another one. Rather, this assumption can be alternatively viewed as a *(H6) mean-field approximation, neglecting fluctuations*: within this approximation, a_0 is in fact a mean rate $\langle \tilde{a}_0 \rangle$, averaged over the whole prey population: $\sum_{i=1}^{X} \tilde{a}_0(i) \approx a_0 X$ if $\tilde{a}_0(i)$ is the reproduction rate of the individual i of the prey population. Note that *(H7) the temporal fluctuations of the rates are also neglected* (average rates over a year, for instance). $W(X-1,Y|X,Y)$ automatically vanishes if $X = 0$ (and similarly $W(X,Y-1|X,Y)$ if $Y = 0$), hence transitions towards negative values of X and Y are forbidden: the dynamics remains in the acceptable set of positive integers for both X and Y. The last step is to deduce:

$$W(X,Y|X,Y) = -\,a_0 X - b_0 XY - c_0 XY - d_0 Y \tag{9}$$

The evolution finally writes:

$$\begin{aligned} \frac{dP(X,Y,t)}{dt} = {} & a_0(X-1)P(X-1,Y,t) - a_0 X P(X,Y,t) \\ & + b_0(X+1)Y P(X+1,Y,t) - b_0 XY P(X,Y,t) \\ & + c_0 X(Y-1)P(X,Y-1,t) - c_0 XY P(X,Y,t) \\ & + d_0(Y+1)(X,Y+1,t) - d_0 Y P(X,Y,t) \end{aligned} \tag{10}$$

Now it is possible to write the evolution of $\langle X \rangle$ and $\langle Y \rangle$:

---

*This memory is related to direct interactions, and should not be confused with the correlation time (a Markov chain can exhibit long-range correlations, in case of near-reducibility of the transition matrix).

$$\frac{d\langle X\rangle}{dt} = a_0\langle X\rangle - b_0\langle XY\rangle \tag{11}$$

$$\frac{d\langle Y\rangle}{dt} = c_0\langle XY\rangle - d_0\langle Y\rangle \tag{12}$$

Here appears the main assumption: identifying $\langle XY\rangle$ with $\langle X\rangle\langle Y\rangle$. It amounts to *(H8) neglects microscopic correlations (hence it involves a second mean-field approximation)*. The justification relies on the law of large numbers and central limit theorem. Actually, the relevant macroscopic variables are not $\langle X\rangle$ and $\langle Y\rangle$, but rather $x = \langle X/N\rangle$ and $y = \langle Y/N\rangle$ where N is some bound on the total population. Whereas $x = \mathcal{O}(1)$, $\langle (X/N)(Y/N)\rangle - xy = \mathcal{O}(1/N)$ decreases with the system size, provided microscopic correlations remain short-range, involving only a (small) fixed number of individuals whatever the size N of the total population is. It shows that the relative influence of the cross-correlation between X and Y is actually negligible when the population size is macroscopic. Note finally that $\langle X\rangle$ and $\langle Y\rangle$ are no longer restricted to integer values, and far more x and y, thus completing the microscopic foundations of the continuous-state macroscopic model (3), with $a = a_0$, $b = b_0N$, $c = c_0N$ and $d = d_0$.

This derivation points out all the different hypotheses and approximations underlying continuous chemical kinetics and similar models; it thus clearly delineate the range of validity of the passage from discrete and stochastic elementary dynamics to a continuous and deterministic one at the scale of the whole population. Accordingly, it hints at situations where this procedure may fail. For instance, finite-size effects are likely to affect chemical kinetic equations: when only a small number of molecules are involved in the reaction, e.g. inside a living cell, it is thus essential to account for the actual discrete and stochastic nature of the variables X, and to investigate the influence of what might be called the "molecular noise", namely the fluctuations $X - \langle X\rangle$ (i.e. $X - Nx$). The consequences of such a noise increase as the system size decreases, setting a minimal size N_{min} below which the original discrete and stochastic description should be used; they are expected to be specially dramatic near bifurcation points of the deterministic continuous kinetic equations, where the minimal size N_{min} takes macroscopic values [Gonze et al. 2002].

Generalization to spatio-temporal systems has attracted much work in theoretical physics and chemical physics, as illustrated in [Arnold 1980] [Chopard and Droz 1998] or [Cardy 2004]. Rigorous mathematical results supporting the above approach and its spatio-temporal analog can be found in [Rezakhanlou 2004].

B. Partitions of the phase space

To account for the finite observation accuracy, say ϵ, available on the system state, it is always possible to replace the original continuous phase space $\mathcal{X}$ by a partition $(\mathcal{X}_{\epsilon,\omega})_\omega$ in cells of linear size ϵ. Nevertheless, starting from a deterministic evolution on $\mathcal{X}$ (discrete in time, i.e. modeled by a map $f : \mathcal{X} \to \mathcal{X}$) such a partition does not always achieves a simplification of the analysis. Indeed, if the partition is arbitrary, the associated discretization typically replaces the deterministic model by a stochastic one, since many trajectories come out a given cell and generally reach several other cells [Givon et al. 2004]. Discretizing the phase space achieves a fruitful reduction of the dynamics to its essential, somehow universal features, in at least two instances (besides related):

— *generating partitions* when by definition the knowledge of the whole sequence $\bar\omega = (\omega_n)_n$ of visited cells specifies a unique point x_0, hence a unique trajectory in the continuous phase space: $\cap_{n\geq 0}\mathcal{X}_{\epsilon,\omega_n} = \{x_0\}$. There is thus no loss of information when describing the evolution at the cell level since $(\omega_n)_{n\geq 0}$ and $(f^n(x_0))_{n\geq 0}$ are uniquely related (except, possibly, for a countable set of points). This is the basic feature underlying *symbolic dynamics* [Lind and Marcus 1995]. For example, the map $f(x) = 2x$ (modulo 1) in $[0,1]$ is equivalent to the *Bernoulli shift* $\bar\omega \to \sigma\bar\omega$ with $(\sigma\bar\omega)_n = \omega_{n+1}$, acting in the space $\{0,1\}^*$ of binary sequences: $\bar\omega(x)$ is the dyadic representation of x: $x = \sum_{i=0}^{\infty} 2^{-(i+1)}\omega_i$. This equivalence is associated with a partition of the phase space in two cells $\mathcal{X}_0 = [0, 1/2[$ and $\mathcal{X}_1 = [1/2, 1[$, namely $\omega_0(x) = 0$ if $x < 1/2$, $\omega_1(x) = 1$ if $x \geq 1/2$, $\omega_n(x) = 0$ if $f^n(x) < 1/2$, and so on [Badii and Politi 1999]:

$$\begin{array}{ccc} x \in [0,1] & \Longrightarrow & \bar\omega \in \{0,1\}^* \\ \downarrow & & \downarrow \\ f(x) & \Longrightarrow & \sigma\bar\omega \end{array}$$

where $\Longrightarrow$ represents the dyadic representation. Such a conjugacy to a Bernoulli shift is a hallmark of fully developed chaos (strong mixing). Work is in progress to extend this viewpoint to multivariate labels (the discrete time n being supplemented with integer labels associated with a partition of real space) in order to get an operational definition of *spatio-temporal chaos*, i.e. chaos occurring in spatially extended systems [Mielke and Zelik 2004].

— *Markov partitions* where by definition[†], the possible successor cells of a given one do not depend on the history (topological Markov property), which is a prerequisite to device a Markov chain modeling at the cell level. In a more stringent instance, that of the so-called Markov maps [MacKernan and Nicolis 1994], the reduction to a Markov model can be done exactly: the symbolic dynamics is a Markov chain, fully characterized by a transition matrix $W_{\omega\omega'} = \mathrm{Prob}(\omega \to \omega')$, with no loss of information compared to the original evolution in the continuous phase space. In other cases, the reduction to a Markov model relies on a *Markov approximation*, supported by the intrinsic stochasticity and memory loss of the underlying evolution in $\mathcal{X}$, if it is sufficiently chaotic, namely mixing [Schnakenberg 1976].

Let us finally add a side remark: as done above, discretization of the phase space is generally performed on a model yet discrete in time. A noticeable exception has been yet encountered in Sec. IV A, with *birth-and-death processes*, that is a Markov chain in $\mathbf{N}^n$ [Gardiner 1983] describing the number, say, of molecules of n different species and involving unit jumps after random waiting times. Another instance of continuous-time and discrete (or countable) state-space process is provided by *Boolean delay equations* [Ghil and Mullhaupt 1985], where the trajectory is an alternation of jumps $0 \to 1$ and $1 \to 0$ at times varying in a continuum.

C. Shannon entropy

The information available about any phenomenon depends upon the observation scale. This obvious statement can be turned into a quantitative tool by exploiting the *notion of (statistical) entropy* introduced by Shannon and allowing to measure the average information gained during the observation. Shannon entropy S is associated with a partition $\mathcal{P} = [\mathcal{X}_i]_{i=1\ldots N}$ of the phase space and a probability distribution $[p_i]_{i=1\ldots N}$ (with $p_i = \mathrm{Prob}[x \in \mathcal{X}_i]$) accounting for the knowledge available prior observation [Shannon 1948]:

$$S(\mathcal{P}, [p_i]_i) = -\sum_{i=1}^{N} p_i \log p_i \tag{13}$$

$\log(1/p_i)$ measures the "surprise" at observing a state $x \in \mathcal{X}_i$ rather than lying in any other cell, hence is taken[‡] as a measure of the information gained by observing the macrostate i. S vanishes if one macrostate i has a probability of 1, whereas it is maximal ($S = \log N$) if the N macrostates are equiprobable. Increasing the resolution, i.e. splitting the cells $(\mathcal{X}_i)_{i=1\ldots N}$ into finer ones leads to an increase of S (since $-(p+p')\log(p+p') \leq -p\log p - p'\log p'$) in agreement with the intuitive statement introducing this section.

It is to note that Shannon entropy is closely related to the entropy encountered in statistical mechanics. The connection between statisical mechanics and information theory has besides been fully developed[§], mainly by Jaynes [Jaynes 1989]. In his seminal works providing the bases of statistical mechanics, Boltzmann adopted a finitist viewpoint through the introduction of a partition of the continuous classical phase space (positions and velocities of all the particles composing the system). The obvious flaw of this approach is the arbitrariness of the partition: in particular, as for the Shannon entropy, the statistical entropy varies when the partition varies. These difficulties encountered in classical statistical mechanics to give an absolute definition of statistical entropy vanish at the quantum level, thanks to the discreteness of the states in a quantum system. Statistical entropy is indeed *univoquely defined in quantum mechanics* according to $S = -\mathrm{Tr}\hat{\rho}\log\hat{\rho}$, where $\hat{\rho}$ is the density matrix [Wehrl 1978]. Coarse-graining procedures can then be developed to relate the full quantum description to classical ones at higher scales. The increase of entropy observed in these procedures reflects the loss of information (about quantum correlations) accompanying the various projections and reduction of the system description involved in the quantum/classical connection [Balian 2004].

[†]For instance, if $\mathcal{X} \subset \mathbf{R}$, f admits a Markov partition $(\mathcal{X}_\omega)_{\omega=1\ldots N}$ if for any $\omega = 1, \ldots, N$, $f(\mathcal{X}_\omega = \cup_{\omega'}\eta_{\omega\omega'}\mathcal{X}_{\omega'}$ where $\eta_{\omega\omega'} = 0$ or 1; we refer to [Guckenheimer and Holmes 1983] for the definition of Markov partitions in higher dimensions.

[‡]This choice $\log(1/p_i)$ as a measure of the information content of the macrostate i (i.e. the set $\mathcal{X}_i$ of microstates) is uniquely prescribed when imposing a relevant behavior for S: continuity, concavity and subadditivity when considering the intersection of two partitions, turning into additivity in case of statistically independent partitions [Wehrl 1978].

[§]Nevertheless, this viewpoint is not shared by the whole community: an alternative, dynamic viewpoint is rather based on the chaotic properties of the microscopic dynamics.

D. ϵ-entropy

Following the line of thought of information theory, and more specifically the above notion of (Shannon)entropy, it is fruitful to introduce a time entropy measuring the information on the starting point x_0 gained when observing its trajectory $(x_j)_{j\geq 0}$ with a *finite resolution* ϵ in the phase space, associated with some partition $[\mathcal{X}_{\epsilon,\omega}]_\omega$. Denoting $\bar{\omega}_n = (\omega_0, \ldots, \omega_{n-1})$ a n-step trajectory observed at this level (by construction $x_j \in \mathcal{X}_{\epsilon,\omega_j}$), we define for each $n \geq 1$ a Shannon-like time entropy

$$H_n(\epsilon) = -\sum_{\bar{\omega}_n} \mathrm{Prob}_n(\bar{\omega}_n) \log \mathrm{Prob}_n(\bar{\omega}_n) \tag{14}$$

The asymptotic rate

$$h(\epsilon) = \lim_{n\to\infty} \frac{H_n(\epsilon)}{n} = \lim_{n\to\infty} [H_{n+1}(\epsilon) - H_n(\epsilon)] \tag{15}$$

is called the ϵ-*entropy* [Kolmogorov and Tikhomirov 1959] [Gaspard and Wang 1993] [Nicolis and Gaspard 1994]. It is thus the rate of information production when observing the evolution with an accuracy ϵ.

This quantity can be defined for both deterministic and stochastic evolutions. It is moreover experimentally accessible [Boffetta et al. 2002]. It charcaterizes the apparent behavior at scale ϵ. For instance, $\lim_{\epsilon\to 0} h(\epsilon) = h_{KS}$ (Kolmogorov-Sinai entropy) in case of deterministic chaos whereas $h(\epsilon) \sim 1/\epsilon^2$ for Brownian motion (normal diffusion). It is thus to be computed prior choosing any modeling. Striking applications of the ϵ-entropy as a tool to describe quantitatively the apparent natures, at different scales, of an actual evolution, are given in [Boffetta et al. 2002]. As yet sketched in Sec. III D on the example of chaotic diffusion, this indicator allows to reconcile models of seemingly different natures (e.g. discrete and continuous) but related through some continuous limit, typically when decreasing some characteristic size a to 0: behaviors at scale ϵ will be the same whatever the value of a, vanishing or not, as soon as $a < \epsilon$. On the contrary, the behavior of $h(\epsilon)$ for $\epsilon < a$ will mark out the difference between the model with $a > 0$ and the limiting, idealized one with $a = 0$. For instance, a behavior $h(\epsilon) \sim 1/\epsilon^2$, in some window for ϵ, supports a stochastic, diffusion-like description at these scales, whatever the actual mechanism at smaller and larger scales.

We have considered here a discrete-time dynamics. The ϵ-entropy can be generalized for continuous-time dynamics into an (ϵ, τ) *entropy* $h(\epsilon, \tau)$, namely the rate of information production when the evolution is observed with an accuracy ϵ and a time-step τ. As for the */epsilon*-dependence, the τ-dependence of $h(\epsilon, \tau)$ is highly meaningful, allowing for instance to discriminate deterministic evolution ($h(\epsilon, \tau) \sim h_{KS}$ for a chaotic dynamics of Kolmogorov-Sinai entropy h_{KS}) and stochastic processes ($h(\epsilon, \tau) \sim (1/\tau)\log(1/\epsilon)$ for a white noise). We refer to [Gaspard and Wang 1993] for a full account on this extended notion and its applications.

As demonstrated in [Falcione et al. 2003], this discussion allows to understand a classical decoherence effect quite similar to the quantum decoherence effect described in [Berry 2001] and [Zurek 1995] (see also Sec. V E). Let us consider a map whose states, i.e. x, are continuous: $x_{k+1} = f(x_k)$ on $[0, 1]$. Let us moreover suppose that the associated dynamics is chaotic, which reflects in a positive Kolmogorov-Sinai entropy $h(f) > 0$). Its discretization with step $a \ll 1$ (discretization in the phase space) writes:

$$z_{k+1} = \mathrm{E}[(1/a) f(a z_k)] \equiv g_a(z_k) \tag{16}$$

where E[.] denotes the integral part. This mapping acts within a finite set of states $\{z_k, k = 0, 1, \ldots, \mathrm{E}[1/a]\}$, hence all trajectories are periodic** (after a possible transient) and the dynamics is non chaotic, which reflects in $h(g_a) = 0$. We here recover the issue, yet encountered in III D, of matching two behaviors of different natures but expected to be indiscernible for all practical purposes when $a \to 0$.

First, it is to note that for $\epsilon > a$, the curve $n \to H_n(\epsilon, g_a)$ follows closely $n \to H_n(\epsilon, f)$ as long as the discretization and ensuing periodicity of the trajectories are imperceptible. This condition puts a bound $n_{max}(a, \epsilon)$ on the observation duration n, that can be estimated as follows: at $n = n_{max}(a, \epsilon)$, the number $\mathcal{N}_n(\epsilon) \sim e^{nh(\epsilon,f)}$ of ϵ-separated trajectories

---

**When the dynamics is periodic of period T, it is straightforward to show that $H_n(\epsilon) = H_T(\epsilon)$ for any $n \geq T$, hence $h(\epsilon) = 0$. The same argument applies here, T being the maximal period of the discrete trajectories (T is actually finite since there is a finite number of discrete states, hence a finite number of discrete deterministic trajectories).

of length n (i.e. trajectories of the continuous system that differ each from each other by a distance at least ϵ at some moment between $t = 0$ and $t = n$) is equal to the number (roughly $1/a$) of discrete states.

$$n_{max}(a, \epsilon) \sim \frac{\log(1/a)}{h(\epsilon, f)} \tag{17}$$

If n_{max} is large enough, the linear part in the curve $n \to H_n(\epsilon, g_a)$ might be enough marked and enough long to estimate $h(\epsilon, f)$ quite correctly. Above n_{max}, the curve $n \to H_n(\epsilon, f)$ tends to the straight line of slope $h(f)$ (i.e. $n^{-1}H_n(\epsilon, f)$ tends to $h(f) > 0$), whereas $H_n(\epsilon, g_a)$ saturates to a constant finite value (roughly equal to $H_{n_{max}}(\epsilon, g_a)$ and of order of $\log(1/a)$, reflecting the periodic regime of the discrete dynamics.

Second, adding an uncorrelated microscopic noise to the discrete evolution might restore the features of the continuous one at large scales $\epsilon \gg a$, exactly as adding noise to a quantum evolution allows to recover the chaotic behavior, if any, of the classical analog. This also can be appreciated on the entropic behavior. Let us consider the case where the noise amounts to uncorrelated random jumps into neighboring a-cells, and let us denote h_{noise} the entropy (rate) of this stochastic process. This noise can be fully appreciated only at scales $\epsilon > a$, and then

$$h(\epsilon, g_a + \text{ noise}) \approx h_{noise} \qquad (\epsilon > a) \tag{18}$$

As shown in [Falcioni et al. 2003], if $h_{noise} \gg h(f)$ and $\epsilon \gg a$, the randomness of the superimposed noise restores the complexity of the chaotic continuous dynamics, namely

$$h(\epsilon, g_a + \text{ noise}) \quad \text{with} \quad a = \alpha\epsilon \quad \text{tends to} \quad h(\epsilon, f) \quad \text{as } \alpha \text{ tends to } 0 \tag{19}$$

The explanation lies in the amplification of the microscopic noise by the deterministic dynamics. In plain words, the dynamic instability still present in the discrete dynamics (before being truncated by the discretization and the ensuing periodicity) feeds on the noise and propagates its randomness (i.e. its entropy) at larger scales, in a way reflecting the underlying continuous dynamics. The random events at scale a allow to bypass the "taming" of chaotic behavior following from the coarse-graining $f \to g_a$, and to recover the full entropic content of the original continuous dynamics at observation scales ϵ large compared to the discretization step $\epsilon \gg a$. The authors finally suggest that chaotic deterministic systems might appear as effective models for randomly perturbed quantum (hence discrete) motion, when observed at classical scales [Falcioni et al. 2003].

The general point to be kept in mind is the *importance of superimposed randomness in the inter-relation between continuous and discrete dynamics*.

V. SPECTRAL ANALYSES

A. Introductory overview of spectral landscape

This heading of "spectral analyses" collects a large variety of notions sharing the name of *spectrum*. The purpose of this section is to give a representative sample of their variety, hence to show that spectral analyses form a whole world, where the alternative between discrete and continuous (here, spectra) is to be enlightened, reflecting deep differences in the behavior of the system, and being possibly richer than a dilemma between only two exclusive possibilities. Here also, a preliminary classification might help. Spectra might correspond to:

— frequencies or, equivalently, time periods (Fourier modes, Sec. V B and power spectrum, Sec. V C);

— wave vectors or, equivalently, wavelengths (spatio-temporal normal modes, Sec. V D, e.g. in pattern formation);

— energy levels, Sec. V E;

— correlation times (i.e. characteristic times for the decay of correlations, Sec. V F);

— amplification rates (Lyapunov exponents, Sec. V G);

— experimentally available spectra and associated spectroscopy methods, Sec. V H.

B. Fourier analysis

Fourier analysis has been introduced by Fourier in 1807 to solve the heat equation $\partial_t T = \chi \Delta T$ for a temperature profile $T(\vec{r})$ [Fourier 1822]. It has since been intensively developed, both on the theoretical side (convergence results,

for instance) and on the practical side (computational methods to implement Fourier transform, for instance Fast Fourier Transform algorithm). I shall not dwell on the basic definitions and properties of Fourier transform but rather discuss its status in the light of the present discrete/continuous debate.

The basic idea is to decompose, say, a real-valued time function $f(t)$ into purely sinusoidal components, namely $A_\omega \cos(\omega t + \phi)$, equivalently $a_\omega \cos(\omega t) + b_\omega \sin(\omega t)$, or in the complex form $\widehat{f}(\omega) e^{i\omega t}$ with $\omega \in \mathbf{R}$. If this function $f(t)$ is T-periodic, it remains only the components with $\omega = \omega_1 \equiv 2\pi/T$ and its harmonics, of frequencies $\omega_n = 2\pi n/T$, turning the continuum of possible frequencies into a discrete set: a discrete, "point spectrum" reveals the periodicity of the associated phenomenon.

Extension to spatio-temporal phenomena is almost straightforward, replacing $e^{i\omega t}$ with $e^{i\omega t - i\vec{q}.\vec{r}}$. A well-known illustration is provided by music instruments: flute, violin strings ($d = 1$) or drum ($d = 2$). In this case, looking for a solution of the wave equation describing the system behavior (e.g. its response to an excitation) relates frequencies ω and wave vectors $\vec{q}$ through a dispersion relation $\omega = qc$ where c is the sound velocity. Boundary conditions (e.g. the deformation of a drum membrane should vanish at its boundary) select only one component (and its harmonics) corresponding to the note emitted by the instrument. Playing the instrument mainly amounts to modulate the boundary conditions to get different notes: this is what achieves a violin player with the fingers of his left hand, tuning the emitted sound by tuning the length of the string section actually excited by the bow. The difference between the different instruments lies in the relative weight of the harmonics, reflecting in the tone and controlled by the way the string is excited (compare a guitar, a violin, a piano and a harpsichord).

Fourier analysis makes sense only in the case of linear equations; it extends to weakly nonlinear equations in a perturbative way, known as *mode coupling theory* [Ma 1976]. Nonlinear terms induce a coupling between components hence generate new frequencies: for instance, the product of $\hat{f}(\omega_1)$ and $\hat{f}(\omega_2)$ contributes to $\hat{f}(\omega_1 + \omega_2)$. It is thus impossible to excite selectively a single frequency (and its harmonics) in a nonlinear system; if a single dominant frequency is observed, its origin lies in the dynamics itself and not in the external influences; we shall detail the emergence of such intrinsic modes in Sec. V D. Finally, we have seen in Sec. II D that time resolution puts bounds on the spectral range that can be scanned experimentally (Nyquist theorem): if the sampling frequency is bounded above by ω_0, only spectral components with $\omega < \omega_0/2$ can be fully determined [Shannon 1949].

C. Power spectrum

Power spectrum is a special instance of Fourier analysis. Given an evolving system, the power spectrum $S_A(\omega)$ of a given observable A is defined as

$$S_A(\omega) = \lim_{T\to\infty} \frac{1}{T} \left| \int_0^T e^{i\omega t}\, A(t)\, dt \right|^2 \tag{20}$$

Much can be seen about the system behavior on this spectrum. For instance, a chaotic behavior is associated with a spectrum having a large bandwidth [Eckmann 1981]. The period-doubling scenario towards chaos is also called "subharmonic cascade" due to the peculiar, dyadic and self-similar structure of the associated spectrum [Lesne 1998]. A quasi-periodic motion (hence of countable spectrum) with three incommensurable frequencies is structurally unstable [Ruelle and Takens 1971], and the weakest perturbation turns it into a chaotic motion associated with a large-bandwidth spectrum. Let us define the auto-correlation[††] function

$$C_A(t) = \lim_{T\to\infty} \left[\int_0^T A(t+s)A(s)\, \frac{ds}{T} - \left(\int_0^T A(t)\, \frac{dt}{T} \right)^2 \right] \tag{21}$$

The Fourier transform of $C_A(t)$ is $\widehat{C}_A(\omega) = \sqrt{2\pi}\ S_A(\omega)$. This result is sometimes called the *Wiener-Khinchine theorem*. Actually, this theorem has a far stronger version, including an ergodic-theoretic aspect: it states the equality of $\sqrt{2\pi} S_A(\omega)$ and $\widehat{\mathcal{C}}(\omega)$ where $\mathcal{C}_A(t)$ is now defined as a statistical correlation function:

[††]Power spectrum and correlation function, as written there, are well-defined only *in the stationary state*; otherwise, one should consider two-time correlation function $C_A(t_0, t)$ for the evolution starting in a given out-of-equilibrium state at time t_0.

$$\mathcal{C}_A(t) = \int A(\varphi_t(x))A(x)\mu(dx) - \left(\int A(x)\mu(dx)\right)^2 \tag{22}$$

where μ is an invariant ergodic[‡‡] measure under the action of the flow $\varphi_t(x)$. One straightforwardly extends the definition of the correlation function $\mathcal{C}_{AB}(t)$ and power spectrum $S_{AB}(\omega)$ to couples of observables (A, B) with $\widehat{\mathcal{C}}_{AB}(\omega) = \sqrt{2\pi}\, S_{AB}(\omega)$. Assuming the existence of an invariant ergodic measure μ, Ruelle and Pollicott have shown that for a class of chaotic systems, $S_{AB}(\omega)$ is meromorphic in a stripe extending on both sides of the real axis, and the position of its poles do not depend on the considered observables A and B. Moreover, these poles are directly related to the asymptotic behavior ($t \to \infty$) of the correlation function (a property of Fourier transform). Complex poles of the power spectrum are thus associated to resonances, the so-called *Ruelle-Pollicott resonances*, and the existence of poles arbitrarily close to the real axis prevent an exponential decay of temporal correlations. Accordingly, mixing requires that all poles lie at a finite distance (bounded below) from the real axis; in this case, they contribute to the correlation decay and their imaginary part provides characteristic times (correlation times) of this decay [Ruelle 1986].

A first kind of singular power spectrum is provided by ‘*continuous singular" spectra*, corresponding to the case when the correlation function do not decay exponentially to 0 but is still integrable (by contrast with the fully correlated periodic dynamics) [Zaks and Pikovsky 2003]. The spectrum is then an intricate superimposition of peaks and large band, i.e. of discrete and continuous features. Such spectra occur in weakly chaotic dynamics exhibiting a divergence of the correlation time, corresponding to the intermittent persistence of regular motion (e.g. laminar transients near an unstable or imaginary fixed point).

Power spectra can exhibit another singular behavior in between discrete and continuous (see Sec. VI D), namely a *power-law behavior*, with no characteristic scale and features at all scales. A celebrated example is turbulence; it involves the real-space analog $E(q)$ of the power spectrum $S(\omega)$ as a function of the wave vector q. Under assumptions of statistical homogeneity, isotropy and stationarity, it satisfies $E(q) \sim q^{-5/3}$ in a wide range of wave vectors q called the inertial range, where eddies at all sizes develop and dissipation is not yet efficient [Frisch 1995].

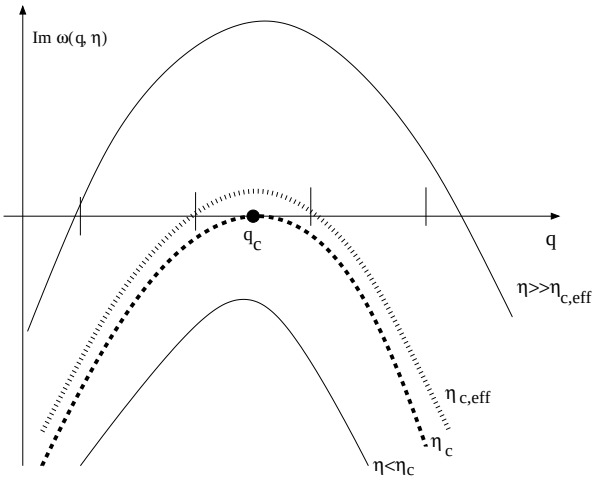

FIG. 9. Dynamic instability and influence of boundary conditions, requiring that $qL \in 2\pi\mathbf{Z}$ (vertical marks on the q-axis); although the instability appears in q_c for $\eta \geq \eta_c$, the actual instability, accounting for boundary constraints, develops only for $\eta \geq \eta_{c,eff}$: spectral selection arises in confined geometry, and might even suppress the dynamic instability.

[‡‡]By definition, the couple (f, μ) of a map $f : \mathcal{X} \to \mathcal{X}$ and a measure μ on $\mathcal{X}$ invariant under the action of f is *ergodic* if and only if any invariant subset $A \subset \mathcal{X}$ is of null or full measure, i.e. $\mu(A) = 0$ or $\mu(\mathcal{X} - A) = 0$ as soon as $f^{-1}(A) = A$. Equivalently, (f, μ) is ergodic if and only if any invariant μ-integrable function φ (i.e. such that $\varphi \circ f = \varphi$ μ-almost everywhere) is μ-almost everywhere constant [Pollicott 1998].

D. Normal modes

Normal mode analysis generalizes Fourier analysis to complex frequencies. It basically amounts to perform a *linear stability analysis* of a uniform stationary state, and to search linear perturbations (solutions of the linearized evolution under the form:

$$a(\vec{q},t)e^{i\vec{q}.\vec{r}} \quad \text{or} \quad A(\omega,\vec{r})e^{-i\omega t} \quad \text{or} \quad \mathcal{A}(\vec{q},\omega)e^{i\vec{q}.\vec{r}i\omega t} \tag{23}$$

yielding a *dispersion relation*

$$\omega = \omega(\vec{q}) \in \mathbf{C} \qquad \text{or more generally} \qquad \mathcal{D}(\omega,\vec{q}) = 0 \tag{24}$$

In a confined medium, $\vec{q}$ is real and "quantified" as required by boundary conditions, e.g. $qL \in 2\pi\mathbf{Z}$ if the underlying space is an interval $[0,L]$ (as seen in Sec. V B, the same constraint rules the Fourier spectrum). The mode is stable if and only if $\mathrm{Im}(\omega(\vec{q})) < 0$. The homogeneous stationary state is thus dynamically stable if and only if $\mathrm{Im}(\omega(\vec{q})) < 0$ for any $\vec{q} \in \mathbf{R}^d$.

For the sake of simplicity, let us consider a unidimensional medium of size L, and the situation where its dynamics depends on a control parameter η. Destabilization occurs at the minimal value η_c such that it exists q_c, with

$$\mathrm{Im}(\omega(\eta_c,q_c)) = 0 \qquad \text{and} \qquad \mathrm{Im}(\omega(\eta_c,q)) < 0 \qquad \text{if} \quad q \neq q_c \tag{25}$$

(see Fig. 9). As soon as $\eta > \eta_c$, a continuum $[q_m(\eta), q_M(\eta)]$ of modes is destabilized, surrounding the value $q_c(\eta)$ where $\mathrm{Im}(\omega(q))$ is maximal. In this window, only those wave vectors satisfying

$$qL \in 2\pi\mathbf{Z} \tag{26}$$

are acceptable. *Although the dynamics allows a continuum of unstable modes*[§§]*, only a discrete set, selected by the boundary conditions, is actually observed.* It is to be underlined that the window of unstable modes is independent of the system geometry: boundary conditions intervene in a second step, as a further selection rule fine-tuning specific modes among the set of dynamically unstable ones. Near the instability threshold, or for small system sizes L, the intersection of $[q_m, q_M]$ with $(2\pi/L)\mathbf{Z}$ might be empty: it means that the instability is hindered by the boundary conditions. As sketched on Fig. 9, the instability can thus be avoided in a confined geometry (L too small) and it develops only if $\eta > \eta_c(L)$ (or equivalently $L > L_c(\eta)$). On the contrary, in a very extended medium ($L \to \infty$, $2\pi/L \ll dq$), the quantification is almost insignificant and in practice, one observes a continuum of unstable modes. All this discussion can be substantiated and illustrated on examples of pattern formation [Cross and Hohenberg 1993], for instance the celebrated Turing structures [Turing 1952]. Spatio-temporal systems thus exhibit the *superimposition of a continuous instability, intrinsically prescribed by the dynamics, and a further selection of discrete modes, imposed by boundary conditions.*

It is to note that a continuous symmetry of the evolution equation induces a marginally stable mode $\omega = 0$. Here again, it appears a kind of conjugacy between continuous features (here a continuous symmetry) and discrete ones (here a mode $\omega = 0$ or $\vec{q} = 0$). Such conjugacy is not an opposition nor a negation but rather a balance, or even a conjunction, where *discrete features exist only when continuous ones are present in the conjugate instance.*

E. Quantum mechanics

Spectral analysis is at the core of quantum mechanics, due to the linear nature of *Schrödinger equation*:

$$\imath\hbar\partial\psi/\partial t = \widehat{H}\Psi \tag{27}$$

and to the Hermitian property of the Hamiltonian operator $\widehat{H}$ acting on the wave function ψ. Eigenvalues $(E_k)_k$ of $\widehat{H}$ correspond to energy levels of the system and associated eigenvectors $(\psi_k)_k$ to "pure states" of well-defined energy E_k. One distinguishes the case of *discrete (or pure point) spectrum*, when the spectrum reduces to the set of eigenvalues;

[§§] The modes are *linearly* unstable; in the true dynamics, nonlinear effects generally induce a saturation of the instability and turn these unstable modes into well-defined structures of bounded amplitude.

the opposite situation is a *continuous spectrum* with no eigenvalues (hence no eigenvectors); the current situation is a *mixed spectrum*, whose restriction to some subspace is a pure point spectrum whereas the complementary part (in the orthogonal, supplementary subspace) is continuous.

The basic idea is that *a discrete spectrum reflects a quantification of the energy*, hence a nonclassical behavior of the system, whereas passing to a continuum marks the energy threshold above which the system behaves classically. Things are nevertheless richer, and a more refined analysis reveals different kinds of continuous spectra, according to their fine structure (related to the existence of "resonances", namely complex poles of the resolvant $[\det (1 - z\widetilde{H}]^{-1}$ of a non-Hermitian extension $\widetilde{H}$ of $\widehat{H}$). This point is fully exposed in the contributions of D. Delande and A. Buchleitner in this volume, in the case of Helium atom.

A quite recently investigated issue is *quantum chaos*. Namely, the issue is to determine whether some specific spectral properties are associated with chaotic properties of the corresponding classical system (limit $\hbar \to 0$, or rather, limit when the ratio $\hbar/A_c$ tends to 0, where A_c is a classical scale for the action) [Gaspard 2004b]. It is to be underlined that *an isolated quantum system does not exhibit chaos*, even if its classical counterpart is chaotic. The reason is that any fine structure (e.g. homoclinic tangle at the origin of chaos, see the contribution by C. Simo in this volume) in the phase space is bounded below at scale $\hbar$. Nevertheless, it can be shown that any external influence, even the weakest one, restore the classical chaotic behavior, a phenomenon belonging to what is called *quantum decoherence*, see for instance the introductory paper [Berry 2001] (see also the classical analog presented in Sec. IV D).

Remarkably, quantum mechanics shows that discrete *vs* continuous issues are multiple and should be precisely delineated to avoid a dialog of the deaf. Indeed, whereas quantum systems appear as the discrete counterparts of classical ones as regards energy spectrum (discrete low-energy levels) and phase space (discrete states), they generally exhibit the opposite behavior in real space: quantum particles are described by continuous, spatially extended wave function, whereas classical ones are localized and described by a few coordinates. This points out that discreteness in phase space[***] and discreteness in real space are not straightforwardly related.

F. Koopman-Frobenius-Perron theory

Spectral analysis also arises in classical mechanics, associated with the *Liouville equation* $\partial_t \rho = L\rho$ for the density $\rho_t(x)$ in the phase space[†††]. This Liouville equation is formally similar to the Schrödinger equation $\partial_t \psi = -\imath \widehat{H}\psi/\hbar$, with the noticeable difference that $\imath\hbar L$ is not Hermitian and ρ is restricted to be a positive function.

The linearity of this Liouville equation should not be misleading: *it does not mean at all that dynamics is linear*; nonlinearities of the dynamics are embedded in the evolution of the phase-space dependence of ρ, i.e. in the evolution of the relative weight of phase space regions which can mix in a complicated nonlinear way as time goes on.

In the case of a discrete time evolution $x_{n+1} = f(x_n)$ in $\mathcal{X} \subset \mathbf{R}^d$, the evolution of the density writes $\rho_{n+1} = P\rho_n$ where the operator P is called the *Frobenius-Perron operator*. P is linear on $L^1(\mathcal{X}, dx)$, positive ($P\rho \geq 0$ if $\rho \geq 0$) and it preserves the L^1-norm of positive integrable functions. An interesting result is the *relation with ergodic theory*: in the case when there exists a stationary density ρ^*, the couple (f, ρ^*) is ergodic if and only if[‡‡‡] $P\rho_n$ is weakly Cesaro-convergent to ρ^*, namely for any initial density ρ_0 and for any bounded measurable function g,

$$\lim_{n\to\infty} \frac{1}{n} \int \sum_{j=0}^{n-1} P^j \rho_0(x) g(x) dx = \int \rho^*(x) g(x) dx \tag{28}$$

[***] Discrete or continuous nature of states, i.e. discrete or continuous nature of the energy spectrum, should not be confused with the bounds following from the Heisenberg uncertainty relations, preventing to observe simultaneously eigenstates for non-commuting observables notwithstanding the discrete or continuous nature of their spectra.

[†††] In case of Hamiltonian dynamics, Liouville equation writes: $\partial_t \rho = L\rho \equiv \{H, \rho\}$ where $\{H, \rho\}$ is the Poisson bracket; it follows that $\rho \equiv 1$ is a stationary solution: Hamiltonian dynamics preserves the phase-space volume, a result known as the *Liouville theorem*.

[‡‡‡] One should add a technical condition on f: it should be non singular with respect to ρ^*, i.e. $\int_{f^{-1}A} \rho^*(x) dx = 0$ for any subset $A \subset \mathcal{X}$ such that $\int_A \rho^*(x) dx = 0$ (namely, the reciprocal image of sets of null measure is also of null measure, for instance, f does not bring an open set onto a point).

If $\mathcal{X}$ is of finite measure, (f, ρ^*) is mixing if $P^n\rho_0$ is weakly convergent for any initial density ρ_0, i.e., for any bounded measurable function g:

$$\lim_{n\to\infty} \int P^n\rho_0(x)g(x)dx = \int \rho^*(x)g(x)dx \tag{29}$$

These statements have a spectral counterpart [Parry 1981] [Pollicott and Yuri 1998]: there exists a stationary density ρ^* if and only if P has an eigenvalue equal to 1 (the eigenvector being then ρ^*); ergodicity follows if and only if this eigenvalue is simple (namely if and only if ρ^* is the unique stationary density of f). If moreover it is an isolated eigenvalue of P, then (f, ρ^*) is mixing. Other eigenvalues are also of interest, since they are associated with characteristic times of the correlation decay. Here appears the close link between Koopman theory and Pollicott-Ruelle resonances (Sec. V C). The Fredholm determinant of P defines the *Selberg-Smale zeta function* $Z(z)$ and the *Ruelle zeta functions* $\zeta_k(z)$:

$$Z(z) = \det(1 - zP) = \prod_k \frac{1}{\zeta_k(z)} \tag{30}$$

Under some technical conditions [MacKernan and Nicolis 1994], the Ruelle zeta functions can be explicitly expressed from the knowledge of all the periodic orbits $\mathcal{O}_j$ (labeled by j)[Gaspard and Dorfman 1995]:

$$\zeta_k(z) = \prod_j \left(1 - \frac{z^{n_j}}{|\Lambda_j|\Lambda_j^{k-1}}\right) \tag{31}$$

where n_j is the period of the periodic orbit $\mathcal{O}_j$ and Λ_j its stability factor, i.e. the product of f' along the orbit, namely $\Lambda_j = f'(x_{j,0})\, f'(x_{j,1}) \ldots f'(x_{j,n_j-1})$. Hence, the decay of time correlations (mixing property) of the dynamics is determined by the dynamic behavior along the periodic orbits; these orbits thus form the skeleton, not only qualitatively but also quantitatively, of the dynamics (see the contribution by C. Simo in this volume). Conversely, the spectrum of P contains the same information, in a somehow integrated form: the inverses of the eigenvalues of U are the poles of $1/Z(z)$ (under some technical restrictions on f). Noticeably, the formula (30) (or rather, its inverse giving the expression of $1/Z(z)$) is strongly reminiscent of the semi-classical *Gutzwiller trace formula* bridging the spectrum of the quantum Hamiltonian and some characteristics (periodic orbits) of the corresponding classical dynamics [Gutzwiller 1990] [Gaspard and Dorfman 1995] (see also the contribution by T. Paul in this volume).

G. Lyapunov spectrum

Given a map f on a compact phase space $\mathcal{X}$ associated with an invariant ergodic measure μ, another spectrum (besides the spectrum of Frobenius-Perron operator and associated Ruelle-Pollicott resonances described above in Sec. V C and Sec. V F) can be considered: the *Lyapunov spectrum*. It is a global feature of the flow, defined as the spectrum of the asymptotic matrix

$$M = \log \lim_{n\to\infty} [\Lambda_n(x)^\dagger \Lambda_n(x)]^{1/2n} \qquad \text{where} \qquad \Lambda_n(x) = Df[f^{n-1}(x)] \circ \ldots \circ Df(x) \tag{32}$$

is the Jacobian matrix iterated along the flow, for any μ-typical x (note that $M(x)$, being invariant under the action of f, is μ-almost everywhere constant due to the ergodicity of (f, μ)). The dynamics is chaotic if and only if this spectrum has a positive part. This positive part *controls the decay of time correlations* due to chaotic amplification of external noise: correlations decay with time t like $\exp[-t \sum (\text{positive Lyapounov exponents})]$. It is to underline that this decay has not the same origin than the decay due to mixing associated with Ruelle-Pollicott resonances (Sec. V C and Sec. V F) [Ruelle 1986]. This sum of positive exponents provides an upper bound on the Kolmogorov-Sinai entropy, where the bound is conjectured to turn into an equality (*Pesin equality*) for a large class of dynamical systems (e.g. hyperbolic Axiom A systems) [Eckmann and Ruelle 1985]. Another conjecture, the *Kaplan-Yorke conjecture*, states that the capacity dimension D_0 (roughly, the fractal dimension of the attractor [Baker and Gollub 1996]) is equal to the Lyapunov dimension

$$d_{Lyap} = j + \sum_{i=1}^{j} \lambda_i/\lambda_{j+1} \tag{33}$$

where j is the integer such that $\sum_{i=1}^{j} \lambda_i \geq 0$ and $\sum_{i=1}^{j+1} \lambda_i < 0$. This statement is proven for a two-dimensional hyperbolic mapping where d_{Lyap} reduces to $1 - (\lambda_1/\lambda_2)$. The total sum of this spectrum (trace of M) gives the *average rate of expansion* (or contraction if negative) of the phase-space volume achieved by the dynamics. In the case of Hamiltonian dynamics, this sum is 0; far more the spectrum satisfies under various additional hypotheses (e.g. constant kinetic energy) a *pairing property* [Dettmann and Morriss 1996]:

$$\lambda_j + \lambda_{2N-j} = 0 \tag{34}$$

where N is the number of degrees of freedom. In the case of extended systems, with many degrees of freedom ($N \gg 1$), it is still an open issue to understand the discrete features of the Lyapunov spectrum, especially the step-like structures observed near $\lambda = 0$ [van Beijeren and Dorfman 1995] [Taniguchi and Morriss 2002]. It is also still in progress to describe generic scaling properties with respect to the number N of degrees of freedom and the possible continuous limit of the spectrum after an appropriate rescaling, e.g. $\widetilde{\lambda}(\alpha) = \lambda(j{=}\alpha N)/\lambda_1$.

H. Experimental spectroscopy

It is not the place even to list the whole variety of spectroscopy methods, from infrared spectroscopy to X-rays (i.e. from low to high energy ranges), including the still developing fluorescence techniques (especially useful in biology to investigate living cell functioning) and more specific probes like circular dichroism (sensitive to structural chirality). Spectroscopy methods roughly separate into two classes: *absorption spectra*, where one records how the system selectively absorbs radiation from incident light, and *emission spectra*, where one records the specific wavelengths radiated by the system. In the two cases, the spectrum profile is related to the atomic structure and degrees of freedom, through the relation $\Delta E = h\nu$ between the photon frequency ν and the energy jump (towards higher energy during absorption and conversely, towards de-excitation and lower energies during emission). For instance, spectroscopy allows to identify elements composing a star from the analysis of its light, or to follow changes in the atomic structure of a macromolecule as some control parameter varies. Its interpretation at larger scale, for instance in terms of conformational changes of the macromolecule, requires a model; this is one of the purposes and achievement of (computer-assisted) molecular modeling.

I. Some conclusions on spectral analyses

Spectral analyses are a powerful way to decompose a given behavior into elementary components, transverse to what can be reached when considering the system at successive instants or when splitting the underlying real space in cells; one besides speaks of "*conjugate space*". The duality discrete/continuous appears quite ill-suited to discriminate spectral properties; indeed:

— discrete spectral values have not the same consequences whether they lie on the real line or in the complex plane;

— continuous spectra may yet be singular (fractal spectra exhibiting a power-law behavior) and their scaling behavior discriminate very different physical behaviors.

The least mathematical analysis underlines that the spectrum of any operator is highly dependent of the functional space in which it operates; in physical words, it depends on the set of observables (in particular prescribed by the geometry and boundary conditions). At the opposite, experimental spectra are unavoidably limited by time resolution (see Sec. V B), noise (50 Hz electric supply, normal modes of the apparatus and less identifiable background noise) and external medium (superimposition of solvent spectral features, for instance).

Some interpretations, e.g. frequencies associated to spectral lines, seem to refer only to discrete spectral features. In fact, we here again encounter some tolerance depending on the observation scale: speaking of "*the* spectral line at a frequency ν_0" makes sense as soon as the width $\delta\nu$ of the peak of the spectrum $S(\nu)$ in $\nu = \nu_0$ is far smaller than the resolution $\Delta\nu \sim \nu^2 \Delta t$ allowed by the experimental setup or computation accuracy. What appears as purely monochromatic peaks might reveal an inner structure when unfolded by a higher resolution. Here also, the discrete or continuous character of a spectrum is an absolute property only for a given mathematical model of the real system, and should be reconsidered, together with its interpretation, when changing the scale of description or observation.

VI. DISCUSSION

A. Singularities

Discreteness is often, if not always, associated with *some kind of singularities*. For instance, any discrete shape A (or concrete body) exhibits a singularity at its boundary (which precisely define the boundary):

$$\mathbf{1}(x) = 1 \quad \text{if} \quad x \in A \qquad \text{and} \qquad \mathbf{1}(x) = 0 \quad \text{if} \quad x \notin A \tag{35}$$

Similarly, any countable partition $(A_j)_j$ (the sets $(A_j)_j$ having pairwise disjoint interiors) can be associated with a stepwise function $f_{|A_j} \equiv j$, discontinuous at each boundary δA_j where it jumps from j to other integer values. We also recover here the leitmotiv of this paper: such a singularity is a *feature of the mathematical idealization* of the system, which is of different nature compared to the smooth "physical" profiles: it physically turns into a smooth step at sufficiently small scales, and into a fuzzy boundary layer at still smaller ones. For all practical purposes, using step functions is to be preferred at larger observation scales (except in the case, discussed in Sec. VI D, of a fractal boundary). *The physical smoothness is nevertheless to be kept in mind to avoid falling into vain paradoxes.*

This point might yet be expressed mathematically, in modeling the boundary by a sigmoidal function

$$f_a(x) = \frac{1}{2}\left[\tanh(x/a) + 1\right] \tag{36}$$

smoothly interpolating between 0 and 1. This profile converges (in the sense of Schwartz distributions) towards a step function in $x = 0$ in the limit when the width a tends to 0 (see Fig. 10):

$$\lim_{a\to 0} \frac{\tanh(x/a)+1}{2} = \lim_{a\to 0} \frac{1}{1+e^{-2x/a}} = \Theta(x) \equiv \begin{cases} 1 \text{ if } x > 0 \\ \\ 0 \text{ if } x < 0 \end{cases} \tag{37}$$

Here, in $d = 1$, the Laplacian Δf_a is merely the second derivative $f_a''(x) = -2\sinh(x/a)\,[a(1+\cosh(x/a))]^{-2}$ which behaves as $-x/2a^3$ in the neighborhood of $x = 0$ (more precisely provided $|x| \ll a$) while remaining bounded when $a \to 0$ at fixed x. Hence the graph of Δf_a exhibits a marked feature, almost diverging to $\pm\infty$ when $a \to 0^{\mp}$, that indicates the steep jump occuring there; the relief of the Laplacian is actually all the more marked as the jump is steep, i.e. as a is small. Taking the limit $a \to 0$ induces a qualitative change: turning the generic situation $a > 0$ (even very small) into the isolated value $a = 0$ is not innocuous. We here recover localization arising in some limit (here $a \to 0$) and associated singularities, reflecting the ideal character and different nature of this representation of a physical boundary. For instance, whereas it makes sense to add a small localized perturbation on the physical profiles and investigate its fate, the only perturbation of a step function (while remaining a step) is a translation of the discontinuity point.

In the above example, as in Sec. III F, Schwartz distributions allow to give a mathematically well-defined meaning to the limit $a \to 0$, and to exchange derivation and limit $a \to 0$, leading to $\Delta\Theta = \delta'$. It is then possible to investigate in an unified framework the stability of a step function with respect to superimposed fluctuations. *Schwartz theory thus reconcile, with all the desired mathematical rigor, discrete and continuous objects* and somehow smoothes out the debate.

More generally, the Laplacian $\Delta f(x)$ measures the difference between the value of f in x and its average in a neighborhood of x. Namely, in $d = 1$

$$\frac{1}{2}\left[f(x+h) + f(x-h)\right] - f(x) \approx \bar{f}_h(x) - f(x) \approx \frac{h^2}{2}\,\Delta f(x) \tag{38}$$

It thus vanishes if f is uniform or linear and it underlines any localized inhomogeneity, bringing out a discrete feature in x from its surrounding $[x-h, x+h]$. In higher dimensions, taking the Laplacian of a shape brings out the discontinuity occurring at its boundaries hence delineates its edges of this shape, providing a basic tool for image analysis [Canny 1986].

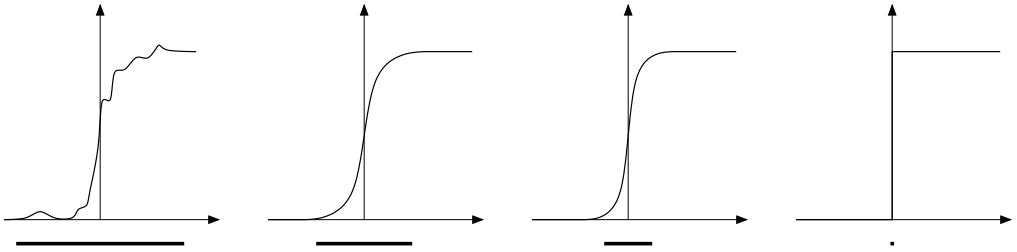

FIG. 10. Sketch of a boundary profile at different scales (the bar indicates a given interval $[-a, a]$). The three smooth profiles, accounting for the same physical feature observed at different scales, are to be contrasted with the mathematical idealization (step-like profile) obtained in the limiting situation $a = 0$.

B. Singular limits and emergent properties

We have just encountered in Sec. VI A a *singular limit* $a \to 0$ and realized the deeply differing nature of the limiting behavior (here a discrete, discontinuous step, see Fig. 10) compared to the behavior for an arbitrarily small but finite value of a (a smooth step). Taking the limit $a \to 0$ induces a *qualitative gap*, from continuous to discrete, since there is no way to recover a smooth profile starting from the discontinuous step. Moreover, the limit is not uniform hence does not commute with other operations (derivation, for instance, or continuous dependence with respect to an auxiliary control parameter) except in the specially designed framework of Schwartz distributions. Such singular limits are ubiquitous in the interplay between discrete and continuous features. Let us cite:

— the continuous limit $\epsilon \to 0$ of a partition in cells of linear size ϵ (or lattice of parameter ϵ),

— the classical limit $\hbar \to 0$ (rather $\hbar/A_c \to 0$ where A_c is the characteristic classical action scale);

— the thermodynamic limit $N \to \infty$.

Paradoxes arise when comparing and trying to relate the properties of finite systems and their limiting behavior [Krivine and Lesne 2003]. It is essential to keep in mind that the limit induces a qualitative change in the system behavior, with an irreversible loss of information. If the system depends on another control parameter θ, it might happen that the limits $\epsilon \to 0$ and $\theta \to \theta_c$ do not commute, as a result of the singular nature of $\epsilon \to 0$. The way out follows from renormalization-group ideas, suggesting to *take jointly the two limits*, according to the procedure: $\epsilon = a\epsilon_1$, $\theta = \theta_c + a^\alpha(\theta_1 - \theta_c)$ and $a \to 0$ at fixed ϵ_1 and θ_1. Typically, the joint limit is trivial except for a special choice of the exponent α, from which we get the full behavior. More generally, joint rescalings often provide a powerful tool to capture singular emergent behaviors [Lesne 1998].

C. Digital computing

Computational mathematics points out the different causal nature of (ideal) digital computing, compared to the standard one, limited by round-off errors [Longo 2002]. In fact, from a physical viewpoint, computing *on actual digital computer* is bound to an accuracy limitation of the same nature: computer elements are physical devices, experiencing external perturbation as well as unavoidable, intrinsic thermal noise (i.e. originating in the thermal motion of atoms, itself merely reflecting their kinetic energy at thermal equilibrium). Strictly speaking, errors can conceivably arise, but practically the probability is so low that they can be considered not to occur. This might be for instance due to a high activation barriers ΔF for taking other paths than the quasi-deterministically prescribed one: the characteristic time to observe the system wandering away can be roughly estimated as the Kramers time $\tau_K \sim e^{\Delta F/k_B T}$ (where k_B is the Boltzmann constant) [Hänggi et al. 1990], and this time increases exponentially if many such barriers line the "deterministic" computation path.

Although impossible to detect in practice, the shade is of importance: *improbability* and *impossibility* are not of the same nature, and no conceptual gap between continuous and digital computing arises if we stick to an improbability of observing another result than the expected one in a digital computation. The same shade is encountered concerning the *emergence of irreversibility* and associated Second Law of thermodynamics; similarly, paradoxes and dead ends appear when treating the improbability (i.e. an event of probability smaller than the inverse age of the Universe) as a strict impossibility (i.e. an event of probability strictly equal to 0) and trying to derive rigorously the microscopic bases of this presumed impossibility of observing backward evolutions [Lebowitz 1993].

Theoretical computing on a Turing machine does not suffer such flaw: it achieves ideal digital computing, hence is of *deeply different causal nature* [Bailly and Longo 2004]. This means that real world does not work as a Turing machine, and that such an ideal machine, on a sufficiently long (but finite) time will always loose the imitation game (proposed by Turing to check the intelligence of machines), if played with an actual physical systems, a human being, or a real computer [Turing 1950]. Only the time required to discriminate the players will vary between these three protagonists of a Turing machine.

D. Fractals: at the border between discreteness and continuity

Fractal geometry, initiated (among others) by Bouligand, Hausdorff and Minkowski (see for instance [Gouyet 1996]) and popularized in physics and other natural sciences by Mandelbrot (see for instance [Mandelbrot 1977a, b]) might be seen as an hybrid of discrete and continuous features.

Let us first recall the definition of the main characteristic of a fractal structure: its *fractal dimension* d_f [Haursdorff 1919]. It might either be local: the mass $M(r)$ contained in a ball of radius r scales according to $M(r) \sim r^{d_f}$, or global: the number $N(\epsilon)$ of cells of linear size ϵ required to cover the fractal structure scales according to $N(\epsilon) \sim \epsilon^{-d_f}$. In the case of a Cantor set (Fig. 11, left), this notion of fractal dimension interpolates between the (integer) topological dimension of the underlying space and the vanishing dimension of discrete (countable) set of points: shall we term discrete (although uncountable) or rather continuous (although of null measure) this Cantor dust? And what about the plane-filling Hilbert curve (Fig. 11, right)? The answer is conditioned by the observer himself: contrary to the case of a usual "Euclidean" body, the local density $\rho(r)$ now depends on the scale r of the observation: $\rho(r) \sim r^{d_f - d}$. In real systems (as the reader might now expect), fractal geometry is an idealization that breaks down at very small scales and very large ones, at which Euclidean geometry rules again.

The fractal structure behaves in practice as a continuum if and only if $d_f = d$ (integer), for instance a Brownian trajectory in the plane or the above-mentioned plane-filling Hilbert curve. In other cases, *fractal structures behave on their own, neither discrete nor continuous, fashion*. They are often the spatial expression of a critical phenomenon, where all scales participate to the behavior and can no longer be separated; accordingly, correlation length ξ diverges. This feature reflects in the self-similarity of fractal structures. The spatial correlation function then exhibits a *power law behavior* $C(r) \sim r^{d_f - d}$ (instead of the exponential decrease $C(r) \sim e^{-r/\xi}$ of finite characteristic scale ξ). In fact, more generally, power laws might be seen as the signature of a *third category lying between discrete and continuous*, yet encountered in spectra in Section V C.

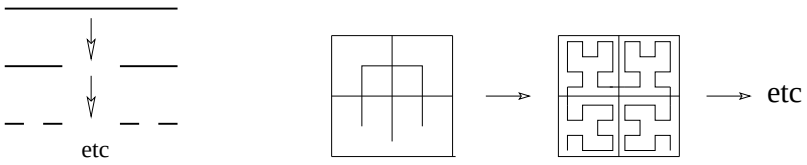

FIG. 11. (Left) lacunary Cantor set, of null measure and fractal dimension $d_f = \log 2 / \log 3$ [Cantor 1883]. (Right) convoluted plane-filling Hilbert curve, with $d_f = 2$ [Hilbert 1891].

Taking the continuous limit might be trivial, e.g. when considering equally distributed discretes tags on a continuous shape or function. It might on the contrary be a puzzling task in the case where this limit is singular, i.e when a qualitative jump arises between the continuous system and its discrete counterparts. A typical example is the measuring of a fractal curve that requires a number of steps of diverging (in case of a convoluted fractal structure with $d_f > 1$) or vanishing total length (in case of a lacunary fractal structure with $d_f < 1$). The way out this puzzle is to rescale jointly the stepsize a and the step number $N(a)$; the exponent involves the fractal dimension $N(ka) \sim k^{-d_f} N(a)$

VII. CONCLUSION

In conclusion, physics in all instances is an interplay between discrete and continuous features, mainly because any such feature actually characterizes a *representation*, from a given observer, of the real system and its evolution. This extended "relativity principle" implies that discrete and continuous modelings, behaviors or computing schemes are the indissociable sides of the same coin. Rather than motivating a debate about the reality of exclusively discrete

or continuous pictures, observations of physical phenomena lead us to elaborate more complex categories, bridging discreteness and continuity: fractal structures, discrete features punctuating a continuum, or continuous behavior smoothing out an accumulation of discrete events. In practice, the choice between discrete and continuous models should be substantiated with the comparison between the respective scales of description, observation, variations (e.g. gradient scales, oscillation periods, or inhomogeneity sizes) and correlations. In this way, it is possible to disentangle, in a "subjective" fashion highly dependent on the specific phenomenon and experimental setup that are considered, the joint discrete and continuous natures of any natural system. It is for instance quite clear nowadays to determine when a photon should be described as a wave or as a punctual particle.

A key point is that *the discrete is not an approximation of the continuum nor the converse*. Great care should be taken when passing from discrete to continuous models and conversely, since their natures are irremediably different. Paradoxes and inconsistencies between discrete and continuous viewpoints only appear when forgetting that our descriptions, and even physical laws, are only *idealized abstractions, tangent to reality in an appropriate scale range*, unavoidably bounded above and below. As a result, wild and spurious features arise when pushing a model beyond its validity range, and limiting behaviors exhibit emergent properties, of qualitatively different nature, reflecting the singularity of the involved limit (continuous limits in the present case). Conversely, coarse-grainings are also quite delicate and care should be taken to get closed effective descriptions, minimizing the loss of relevant information and approximations. But both procedures (continuous limits and coarse-grainings) are at the core of theoretical physics, aiming at unifying all the different observations, descriptions and laws into a consistent, minimal hence explanatory frame, capturing the multiple facets of real world.

This point is subsumed in a more general one: any physical theory is in the same way based on a representation of the system and deals only with this representation, while the reality always remains beyond and is never fully captured. Hence, as yet underlined by Newton, and more recently in the context of irreversible thermodynamics [Chernov and Lebowitz 1997], the mathematical analysis of any physical model should be enlarged with an additional pragmatic status for the ensuing assertions, that of being *physically exact*. Indeed, since the model is only a plausible approximation of the real system, only robust and plausible features make sense, hence some tolerance on improbable events should be accepted: a property that fails to be observed only with a negligible property (at relevant scales) should be considered as true. *This opens a gap between mathematics and physical studies, which is essential to go beyond the mere analysis of a model and shift to the understanding of real world.*

Acknowledgements: I wish to thank warmly M. Falcione, H. Krivine, G. Longo, J. Treiner, and A. Vulpiani for numerous fruitful discussions and their comments on a preliminary version of this paper.

VIII. REFERENCES

Arnold, L. (1980). On the consistency of the mathematical models of chemical reactions, in *Dynamics of synergetic systems*, edited by H. Haken, Springer, Berlin, pp. 107–118.

Auger, P. and Roussarie, R. (1994). Complex ecological models with simple dynamics: From individuals to populations, *Acta Biotheoretica* **42**, 111–136.

Bailly, F. and Longo, G. (2004). Causalités et symétries dans les sciences de la nature. Le continu et le discret mathématiques, in *Logique et interaction: pour une géométrie de la cognition*, edited by J.B. Joinet, Presses Universitaires de la Sorbonne, Paris.

Balian, R. (2004). Entropy, a protean concept, in *Poincaré Seminar 2003*, edited by J. Dalibard, B. Duplantier and V. Rivasseau, Birkhaüser, Basel.

Baker, G. L. and Gollub, J. B. (1996). *Chaotic dynamics: An introduction*, 2nd ed. Cambridge University Press.

Badii, R. and Politi, A. (1999). *Complexity. Hierarchical structures and scaling in physics*, Cambridge University Press.

Bensoussan A., Lions, J.L., and Papanicolaou, G. (1978). *Asymptotic analysis for periodic structures*, North Holland, Amsterdam.

Berry, M. (2001). Chaos and the semiclassical limit of quantum mechanics (is the moon there when somebody looks?), in *Quantum mechanics: Scientific perspectives on Divine Action*, edited by R.J. Russell, P. Clayton, K. Wegter-McNelly and J. Polkinghorne, Vatican Observatory – CTNS Publications, pp. 41–54.

Boffetta, G., Cencini, M., Falcioni, M., and Vulpiani, A. (2002). Predictability: a way to characterize complexity, *Phys. Rep.* **356**, 367–474.

Canny J.F. (1986). A computational approch to edge detection, *IEEE Transactions on Pattern Analysis and Machine Intelligence* **8**, 679–714.

Cantor G. (1883). Über unendliche, lineare Punktlannigfaltigkeiten, *Mathematische Annalen* **21**, 545–591.

Cardy, J. (2004). *Field theory and nonequilibrium statistical mechanics*, lecture notes available online, (http://www.thphys.physics.ox.ac.uk/users/JohnCardy/home.html).

Chernov, N. and Lebowitz, J.L. (1997). Stationary nonequilibrium states in boundary driven Hamiltonian systems: shear flow, *J. of Stat. Phys.* **86**, 953–990.

Chopard, B. and Droz, M. (1998). *Cellular automata modeling of physical systems*, Cambridge University Press.

Cross M.C. and Hohenberg, P.C. (1993). Pattern formation outside of equilibrium, *Revs. Mod. Phys.* **65**, 851–1112.

Dettmann, C.P. and Morriss, G.P. (1996). Proof of Lyapunov exponent pairing for systems at constant kinetic energy, *Phys. Rev. E* **53**, R5545–R5548.

Diener, F. and Diener, M., eds. (1995). *Nonstandard analysis in practice*, Springer, Berlin.

Dorfman, J.R. (1999). *An introduction to chaos in nonequilibrium statistical mechanics*, Cambridge University Press.

Droz, M. and Pekalski, A. (2004). Population dynamics with or without evolution: a physicist's approach, *Physica A* **336**, 84–92.

Eckmann, J.P. (1981). Roads to turbulence in dissipative dynamical systems, *Revs. Mod. Phys.* **53**, 643–654.

Eckmann, J.P. and Ruelle, D. (1985). Ergodic theory of chaos and strange attractors, *Revs. Mod. Phys.* **57**, 617–656.

Ernst, M.H. (2000). Kinetic theory of granular fluids: hard and soft inelastic spheres, in *Proc. NATO ASI on dynamics: models and kinetic methods for non-equilibrium many body systems*, edited by J. Karkheck, Kluwer, Dordrecht, pp. 239–266.

Falcioni, M., Vulpiani, A., Mantica, G., and Pigolotti, S. (2003). Coarse-grained probabilistic automata mimicking chaotic systems, *Phys. Rev. Lett.* **91**, 044101.

Frisch, U. (1995). *Turbulence : The legacy of A.N. Kolmogorov*, Cambridge University Press.

Gardiner, C.W. (1983). *Handbook of stochastic methods* Springer-Verlag, Berlin.

Gaspard, P. (2004a). Maps, in *Encyclopedia of Nonlinear Science*, edited by A. Scott, Taylor & Francis, London.

Gaspard, P. (2004b). Quantum theory, in *Encyclopedia of Nonlinear Science*, edited by A. Scott, Taylor & Francis, London.

Gaspard, P. and Dorfman, J.R. (1995). Chaotic scattering theory, thermodynamic formalism and transport coefficients, *Phys. Rev. E* **52**, 3525–3552.

Gaspard, P. and Wang, X.J. (1993). Noise, chaos, and (τ, ϵ)-entropy per unit time, *Phys. Rep.* **235**, 321–373.

Ghil, M. and Mullhaupt, A. (l985). Boolean delay equations: periodic and aperiodic solutions, *J. Stat. Phys.* **41**, l25–l74.

Givon, D., Kupferman, R., and Stuart, A. (2004). Extracting macroscopic dynamics: model problems and algorithms, *Nonlinearity* **17**, R55–R127.

Gonze, D., Halloy, J, and Gaspard, P. (2002). Biochemical clocks and molecular noise: Theoretical study of robustness factors, *J. Chem. Phys.* **116**, 10997–11010.

Gouyet, J.J. (1996). *Physics and fractal structures*, Springer, New York.

Gruber, C., Pache, S., and Lesne, A. (2004). The Second Law of thermodynamics and the piston problem, *J. Stat. Phys* **117**, 739–772.

Guckenheimer J. and Holmes, P. (1983). *Nonlinear oscillations, dynamical systems and bifurcations of vector fields*, Springer, Berlin.

Gutzwiller, M.C. (1990). *Chaos in classical and quantum mechanics*, Springer, New York.

Hänggi, P., Talkner P., and Borkovec, M. (1990). Reaction-rate theory: fifty years after Kramers, *Revs. Mod. Phys.* **62**, 251–341.

Hausdorff F. (1919). Dimension und ausseres Mass, *Math. Ann.* **29**, 157–179.

Hilbert D. (1891). Über die stetige Abbildung einer Linie auf ein Flächenstück, *Mathematische Annalen* **38**, 459–460.

Jaynes, E.T. (1989). *Papers on probability, statistics and statistical physics*, Kluwer, Dordrecht.

Kirkpatrick, T.R. and Ernst, M.H. (1991). Kinetic theory for lattice gas cellular automata, *Phys. Rev. A* **44**, 8051–8061.

Kolmogorov, A.N. and Tikhomirov, V.M. (1959). ϵ-entropy and ϵ-capacity of sets in functional space, *Russian Mathematical Surveys* **2**, 277–364. Translated in *Translations Am. Math. Soc.* **17**, 277-364 (1961). Available pp. 86-170 in *Selected works of A. N. Kolmogorov*, Vol. III, edited by A.N. Shiryayev, Kluwer, Dordrecht (1993).

Krivine, H. and Lesne, A. (2003). Mathematical puzzle in the analysis of a low-pitched filter, *American Journal of Physics* **71**, 31–33.

Laguës, M. and Lesne, A. (2003). *Invariances d'échelle*, Series "Échelles", Belin, Paris.

Landau, L.D. and Lifschitz, E.M. (1984). *Theory of elasticity*, Pergamon Press, Oxford. *Hydrodynamics*, Pergamon Press, Oxford. *Electromagnetism of continuous media*, Pergamon Press, Oxford.

Lebowitz, J.L. (1993). Boltzmann's entropy and time's arrow, *Physics Today* **46**, 32–38.

Lesne, A. (1998). *Renormalization methods*, Wiley, New York.

Lind, D and Marcus, B. (1995). *An introduction to symbolic dynamics and coding*, Cambridge University Press.

Longo, G. (2002). Laplace, Turing and the "imitation game" impossible geometry: randomness, determinism and program's in Turing's test, in *Conference on cognition, meaning and complexity*, Univ. Roma II, June 2002.

Ma, S.K. (1976). *Modern theory of critical phenomena*, Benjamin, Reading.

Mac Kernan, D. and Nicolis, G. (1994). Generalized Markov coarse-graining and spectral decompositions of chaotic piecewise linear maps, *Phys. Rev. E* **50**, 988–999.

Mandelbrot B. (1977a). *Fractals: form, chance and dimension*, Freeman, San Francisco.

Mandelbrot B. (1977b). *The fractal geometry of Nature*, Freeman, New York.

Mielke, A. and Zelik, S. (2004). Infinite-dimensional hyperbolic sets and spatio-temporal chaos in reaction-diffusion systems in $\mathbf{R}^n$ (preprint available at http://www.iadm.uni-stuttgart.de/LstAnaMod/Mielke).

Murray J.D. (2002). *Mathematical biology*, 3rd edition, Springer, Berlin.

Nicholson, C. (2001). Diffusion and related transport mechanisms in brain tissue, *Rep. Prog. Phys.* **64**, 815–884.

Nicolis, G. and Gaspard, P. (1994). Toward a probabilistic approach to complex systems, *Chaos, Solitons and Fractals* **4**, 41–57.

Nyquist, H. (1928). Certain topics in telegraph transmission theory, *AIEE Trans.* **47**, 617–644.

Parry, W. (1981). *Topics in ergodic theory*, Cambridge University Press.

Poincaré, H. (1892). *Les méthodes nouvelles de la mécanique céleste*, Gauthiers-Villars, Paris.

Pollicott, M. and Yuri, M. (1998). *Dynamical systems and ergodic theory*, Cambridge University Press.

Rezakhanlou, F. (2004). *Kinetic limits for interacting particle systems*, Lecture Notes in Mathematics, Springer, in press.

Ruelle, D. (1986). Resonances of chaotic dynamical systems, *Phys. Rev. Lett.* **56**, 405–407.

Ruelle, D. and Takens, F. (1971). On the nature of turbulence, *Commun. Maths. Phys.* **20**, 167–192; *Commun. Maths. Phys.* **23**, 343–344.

Schnakenberg, J. (1976). Network theory of microscopic and macroscopic behavior of master equation systems, *Revs. Mod. Phys.* **48**, 571–585.

Shannon, C.E. (1948). A mathematical theory of communication, *The Bell System Technical Journal* **27**, 479–423 and 623–656.

Shannon, C. (1949). Communication in the presence of noise, *Proceedings of the IRE* **37**, 10–21. Reprinted in *Proceedings of the IEEE* **86**, 447–457 (1998).

Stauffer, D. and Aharony, A. (1992). *Introduction to percolation theory*, Taylor & Francis, London.

Taniguchi, T. and Morriss, G.P. (2002). Stepwise structure of Lyapunov spectra for many-particle systems using a random matrix dynamics, *Phys. Rev. E* **65**, 056202.

Thomas, R., Kaufman, M. (2001). Multistationarity, the basis of cell differentiation and memory. I. Structural conditions of multistationarity and other non-trivial behaviour. II. Logical analysis of regulatory networks in terms of feedback circuits, *Chaos* **11**, 170–195.

Turing, A.M. (1950). Computing machinery and intelligence, *Mind* **59**, 433–560.

Turing, A.M. (1952). The chemical basis of morphogenesis, *Phil. Trans. R. Soc. London B* **237**, 37–72, reprinted in *Collected works of A.M. Turing*, vol. 2, edited by P.T. Saunders, North Holland, Amsterdam (1992).

Van Beijeren, H. and Dorfman, J.R. (1995). Lyapunov exponents and Kolmogorov-Sinai entropy for the Lorentz gas at low densities. *Phys. Rev. Lett.* **74**, 1319–1322.

Vicsek, T., ed. (2001). *Fluctuations and scaling in biology*, Oxford University Press.

Werhl, A. (1978). General properties of entropy, *Rev. Mod. Phys.* **50**, 221–260.

Zaks, M. and Pikovsky, A. (2003). Dynamics at the border of chaos and order, in *The Kolmogorov legacy in physics*, edited by R. Livi and A. Vulpiani, pp. 61–82.

Zurek, W.H. and Paz, J.P. (1995). Quantum chaos: a decoherent definition, *Physica D* **83**, 300–308.

Contents